

Quantifying information transfer and mediation along causal pathways in complex systems

Jakob Runge

Potsdam Institute for Climate Impact Research, P.O. Box 60 12 03, 14412 Potsdam, Germany

(Dated: July 17, 2022)

Measures of information transfer have become a popular approach to analyze interactions in complex systems such as the Earth or the human brain from measured time series. Recent work has focused on causal definitions of information transfer excluding effects of common drivers and indirect influences. While the former clearly constitutes a spurious causality, the aim of the present article is to develop measures quantifying different notions of the strength of information transfer along indirect causal paths, based on first reconstructing the multivariate causal network (*Tigramite* approach). Another class of novel measures quantifies to what extent different intermediate processes on causal paths contribute to an interaction mechanism to determine pathways of causal information transfer. A rigorous mathematical framework allows for a clear information-theoretic interpretation that can also be related to the underlying dynamics as proven for certain classes of processes. Generally, however, estimates of information transfer remain hard to interpret for nonlinearly intertwined complex systems. But, if experiments or mathematical models are not available, measuring pathways of information transfer within the causal dependency structure allows at least for an abstraction of the dynamics. The measures are illustrated on a climatological example to disentangle pathways of atmospheric flow over Europe.

I. INTRODUCTION AND BRIEF REVIEW

The availability of vast amounts of time series data from such complex systems as the Earth or the human brain and body has given rise to a plethora of time series analysis methods aimed at understanding interactions between regions or subprocesses in these complex systems. Of a particular interest are methods to quantify some notion of *information flow* or *information transfer* within the complex system. In neuroscience [1] and climate research [2, 3], such interpretations have often been based on pure pairwise correlation analyses. But towards measuring information transfer, the method should, firstly, be general enough to include also nonlinear associations. This can be achieved in an information-theoretic framework with measures such as mutual information (MI) [4]. Secondly, networks reconstructed from pairwise measures of association (be it cross-correlation or MI) do not allow to assess the propagation of information or hypothetical perturbations in a causal sense: For example, an interaction like $X \leftarrow Z \rightarrow Y$ would imply that X and Y are correlated even though no perturbations originating in X can actually reach Y , or vice versa.

An important step towards deeper insights has, therefore, been achieved by methods that are capable of inferring a statistical notion of directionality or even causal interactions which have been applied to the climate system [5–10], the human brain [11–13], and to disentangle cardiovascular processes [14–16], among others. Causal associations between subprocesses can be visualized as links in a complex interaction network. A full causal reconstruction of a link $X \rightarrow Y$ can only be achieved under the in most cases unrealistic assumption that all possible other influences on X and Y can be included in the analysis [17, 18], or if the system can be experimentally manipulated within Pearl’s causal effect framework [19]. Usually, it is impossible to exclude all other influences and large complex systems can typically not be easily experimentally manipulated. Causal inference based on data-analysis methods, therefore, provides only a first step and the term “causal” can then only be understood to be meant relative

to the system under study, i.e., the processes that comprise the nodes of the network.

Two tasks need to be addressed to measure a causal notion of information transfer from time series of complex systems:

1. Reconstructing the causal network,
2. Quantifying causal information transfer.

In this article we will only briefly discuss the reconstruction problem, which has been addressed in Ref. [20], and focus on the quantification. As further reviewed below, previous works have mainly considered a decomposition of the predictive information in direct drivers of a process Y . In the present article, we ask a different question: How does information *originating* in a process X propagate through the causal interaction network? How strong is it and which pathways are contributing to such a mechanism?

The paper is organized as follows: In the remainder of this introductory section, we review recent approaches to measuring information transfer in complex systems and sketch the basic idea underlying the present approach. In Sect. II we recall basic concepts of information theory and in Sect. III define *time series graphs* and briefly discuss their reconstruction as the causal basis of the present approach. In Sect. IV we define interaction measures from the well-known lagged MI to novel measures based on time series graphs to quantify interactions along paths and mediation. In Sect. V we extensively analyze the measures with analytical and numerical examples and provide theorems that foster a more rigorous mathematical and dynamical understanding to facilitate the interpretability of the proposed measures. Section VI discusses the theoretical results and relation to linear measures of causal effect in Pearl’s framework [21], and gives an outlook to applications of the novel measures in complex network theory. Finally, Sect. VII gives an illustrative application to climatological time series and Sect. VIII concludes the paper. The appendix contains proofs of the theorems.

A. Reconstructing the causal network

Considering a multivariate definition of causality, a plethora of methods exists that implement the model-based concept of Granger causality [17]. These range from classical linear autoregressive models in the form of the *directed transfer function* [22–24], to slightly less restrictive approaches such as *partial directed coherence* using spectral estimators [25–29], *extended Granger causality* with local linear embeddings in phase space [30], or kernel estimators [31], to name just a few. All these approaches still involve strong assumptions about the dependencies and share the problem that the model might be misspecified. Information-theoretic approaches that capture almost any form of statistical association are much more difficult to estimate if more than a few variables are involved. Measures such as *transfer entropy* (TE) [32] as discussed in Refs. [13, 33–36], have, thus, mainly been applied in a bivariate setting. A typical approach to uncover coupling delays in bivariate systems (assuming that no common driver is relevant) used in Refs. [34, 37] with a certain lag-specific TE and in Ref. [38] with a *bivariate ordinal pattern momentary information transfer* (which is different from the multivariate version used here and in Ref. [39]) is to determine coupling lags from peaks of the lag-function. As discussed in Ref. [34], however, the bivariate MIT might peak at the wrong lag while, on the other hand, also the bivariate lag-specific TE used in Ref. [34] fails if more than one coupling delay exists between the two processes [40]. In both cases the problem is that more complex couplings require to exclude more possible confounders by conditioning. The main problem with multivariate extensions of transfer entropy (*conditional* or *partial* or *multivariate transfer entropy*) is that one cannot simply condition on as many as possible other variables due to the curse of dimensionality [20]. A multivariate causal reconstruction, therefore, necessitates an iterative procedure.

Several algorithms have been proposed in recent years, e.g., based on a forward-selection algorithm to reconstruct causally predictive variables, called *non-uniform embedding* in Refs. [14, 15, 36, 41] or *optimal causation entropy* in Refs. [42–44], and subsequently testing for causal drivers conditional on this predictive set, similar to backward-elimination. The important question is what the result of such an algorithm is, i.e., to what causal network the algorithm converges. In this work, we base the definition of a multivariate causal network in the framework of *graphical models* [45], also called *time series graphs* for time-ordered data [20, 46] as defined in Sect. III. These encode the Markovian conditional independence relations of a multivariate process, i.e., how the joint density of the whole process (and its lags) factorizes. Graphical models can be estimated by causal discovery algorithms such as Pearl’s inductive causation algorithm [19, 47] or with more efficient versions such as the PC algorithm (named after its inventors Peter Spirtes and Clark Glymour [18, 48]). The conditional independence tests in the PC algorithm can be implemented in a linear framework with partial correlation [49, 50], but a notion of more general information transfer necessitates non-parametric information-

theoretic estimators, e.g., based on nearest-neighbors [51, 52], as implemented in the causal algorithm proposed in Ref. [20]. The consistency of this causal algorithm to converge to the true underlying time series graph under certain assumptions as discussed in Sect. III is proven in Ref. [18]. Note that a pure forward-selection algorithm can, in general, not be used to reconstruct graphical models as discussed in Appendix A and must be combined with a backward-elimination scheme to remove spurious drivers. In Sect. III we briefly discuss some aspects and limitations of causal algorithms, but a thorough comparison of the different algorithms mentioned above regarding their underlying assumptions, statistical power, consistency, and computational complexity is beyond the scope of this work.

B. Quantifying causal information transfer

The second task of quantifying causal information transfer is much more difficult and ambiguous to define in a universal way which has led Smirnov [53] to question the goal of assessing a “causal coupling strength” and instead measure “how the coupling manifests itself in the dynamics” in an *interventional-effect* causal framework as proposed by Pearl [19]. In Ref. [33] the term ‘information transfer’ is even distinguished from ‘information flow’ where the latter is meant in a causal sense based on interventions. This framework, however, necessitates either to experimentally manipulate the system, or to have a mathematical model to perform “virtual interventions”. To some extent causal effects can also be extracted if the time series cover the whole state of the complex system [53] such that virtual interventions can be drawn ‘randomly’ from the stationary distribution.

Generally, however, especially in large spatio-temporal systems such as the Earth or the human brain, mathematical models are either not available or computationally expensive and may not adequately represent important interactions such as the complicated interplay between El Niño Southern Oscillation and the Indian Monsoon in the climate system [54] or neural interactions where even a fully physical model is lacking. If it is not possible to measure “how the coupling manifests itself in the dynamics”, information-theoretic quantifiers can at least help to measure “how the causal coupling manifests itself in the exchange of entropy between the subprocesses” in an information-theoretic framework, where ‘causal’ is meant relative to the observed process as discussed above. This approach aims to distinguish different contributions based on the Markovian conditional independence structure of the multivariate process as an abstraction of the dynamics.

There are few works considering multivariate definitions of information transfer and their interpretation. In Ref. [36], the central concept is to decompose the predictive information about the next time step of a subprocess Y into the MI between Y and its own past as the *information storage*, the *partial transfer entropy* from another subprocess X , and the TE between Y and the remaining process. Liang [55, 56] presents a rigorous approach based on the underlying Langevin de-

scription of a system to define the contributions of internal and external driving to the evolution of the entropy of a subprocess Y . This approach is, however, based on the knowledge of the deterministic-stochastic equations of the system, but in principle it can also be estimated from time series alone involving numerical optimization problems. In Refs. [57, 58] an idea is described that is similar to the present approach in that there the question of quantifying the strength of links is seen as a second step based on the known causal network. Ay *et al.* [57] address the problem from an interventionist perspective using Pearl's do-calculus [19] which we do not further discuss here since we assume the process to be not manipulable. Janzing *et al.* [58] define the strength of a link $X \rightarrow Y$ by considering the thought experiment of an attacker 'cutting the link' and feeding in the distribution of X as an input, arriving at a measure that is not a conditional mutual information anymore, which we use here to measure the transfer of information. Also, the authors state that it is difficult to quantify also indirect effects in their framework. In general, there are different ways to define measures and different research questions demand different properties.

In previous work [39], a set of properties was proposed to arrive at a *well-interpretable* notion of causal strength. These are that the measure should be *lag-specific*, *causal*, *practically estimable*, and have the property of *coupling strength autonomy*. The property of causality in Ref. [39] was excluding indirect links such as $X \rightarrow W \rightarrow Y$. In the present work, we generalize this approach: How does information originating in a process X propagate through the causal interaction network? How strong is it and which pathways are contributing to such a mechanism? In this context the property of coupling strength autonomy demands that the measure should be uniquely determined by the interaction of the two or more processes, (X, W, Y) in the previous example, alone and in a way autonomous of how these are driven by the remaining processes. To understand this, consider a simple example: Suppose we have two interacting processes X and Y and a third process Z , that drives both of them. Then a bivariate measure of coupling strength between X and Y such as MI will be influenced by the common input of Z , while our demand is, that the measure should be autonomous of the interactions of X and Y with Z . The concept of *momentary information* originating in a process X [39] implements this property and is the central idea of the measures introduced in this article. These measures, thus, complement alternative decomposition approaches such as in Refs. [36, 55] as further discussed in Sect. I C.

In summary, this paper generalizes the idea underlying [39] to use the reconstructed causal network for quantifying general causal interactions. This framework is called the *Tigramite* approach (*Time series graph based Measures of Information Transfer*), which is also the abbreviation of the accompanying software package (available on the author's website).

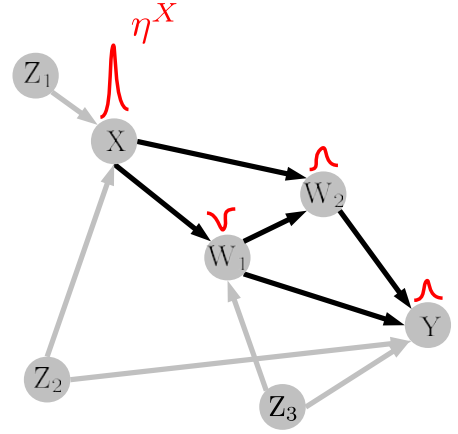


Figure 1. Consider a realization of dynamical noise η^X driving subprocess X as a perturbation. Coupling mechanisms along different causal paths (black lines) transform such a perturbation, and the total effect on Y some time later can also depend on how intermediate processes nonlinearly interact with each other as shown in Sect. V B. The central idea of the momentary information transfer measures presented in this article is to information-theoretically quantify the general effect of such perturbations and isolate it from common drivers in the past such as Z_2 , but also Z_1 and the past of X . To also quantify how much intermediate processes such as (W_1, W_2) on causal paths mediate information, it will also be important to exclude common drivers like Z_3 .

C. The idea of momentary information

The approach to measures of causal information transfer formally introduced in Sect. IV is based on the fundamental concept of *source entropy*, also termed the *entropy rate* [59, 60], and was introduced for the special case of bivariate ordinal pattern time series in Ref. [38]. Consider a symbol-generating process X . At each time t a realization x_t is generated. Now the source entropy of X_t measures the uncertainty about x_t before its observation if all former observations $(x_{t-1}, x_{t-2}, \dots)$ are known (entropies will be formally introduced in Sect. II). For a completely deterministic non-chaotic system the source entropy will always be zero, but for a real world process there will always be some uncertainty stemming from *dynamical noise*. This type of noise is to be distinguished from *observational noise* which usually contaminates each measured time series [61], but has no effect on the dynamics of the process. Dynamical noise might occur due to unresolved smaller-scale processes and can be modeled by including a random variable in the system. More formally, consider a subprocess X of a multivariate process \mathbf{X} with infinite past $\mathbf{X}_t^- = (\mathbf{X}_{t-1}, \mathbf{X}_{t-2}, \dots)$, that is described by the discrete-time equation

$$X_t = f(Z_{1,t-\tau_1}, Z_{2,t-\tau_2}, \dots, \eta_t^X), \quad (1)$$

with some arbitrary function f of other subprocesses at past times $Z_{1,t-\tau_1}, Z_{2,t-\tau_2}, \dots \in \mathbf{X}_t^-$ and the random part subsumed under η_t^X . The uncertainty of an outcome

x_t will *on average* be reduced if a realization of the past $Z_{1,t-\tau_1}, Z_{2,t-\tau_2}, \dots$ is known. But for non-zero η_t^X there will always be some “surprise” left when observing x_t . This surprise gives us information and the expected information here is the source entropy $H(X_t|\mathbf{X}_t^-)$ of X . If the dynamical noise η_t^X occurs additively in Eq. (1), then $H(X_t|\mathbf{X}_t^-) = H(\eta_t^X)$. Due to measurement errors or observational noise ϵ , we will in general not be able to estimate the source entropy alone, but only $H(X_t + \epsilon_t^X|\mathbf{X}_t^- + \epsilon_t^X)$. Even assuming a perfect measurement apparatus for a deterministic dynamical system without dynamical noise, the entropy rate h^{symp} – since it is computed by creating a symbol sequence from a coarse graining in phase-space – depends on some resolution parameter r . Then the limit $\lim_{r \rightarrow 0} h^{\text{symp}}$ might exist and is called the *Kolmogorov-Sinai entropy*. If this limit is finite and larger than zero, the system is called chaotic. But here we study stochastic, discrete time processes because the finite set of measured variables of a complex system like the Earth will never perfectly describe the full system’s state and all remaining processes contribute to dynamical noise (implying that the Kolmogorov-Sinai entropy diverges).

While the focus in Ref. [36] and related works is on decompositions of predictive information on the basis of transfer entropy as an information-theoretic generalization of Granger causality, the concept here is more similar to *Sims* causality, see, e.g., [62], which takes into account not only direct, but also indirect causal effects. Sims causality is based on measuring to what extent X at time t helps in predicting Y at times $t' > t$ in the future excluding the past of X and also the present of all other processes, i.e., $\mathbf{X}_{t+1}^- = (\mathbf{X}_t, \mathbf{X}_{t-1}, \dots)$. In model (1) excluding the past essentially isolates the dynamical noise η_t^X and our goal is now to quantify the information transfer emanating from η_t^X into the future (Fig. 1). With this central idea we define several measures that allow to quantify the interaction between two causally linked processes, but also along causal paths and the mediation of intermediate processes, which can have an explaining, but also a counteracting effect as we discuss in examples.

Pearl [19] defines the causal effect of X on Y by the hypothetical intervention of *experimentally setting* a variable X to a certain value x . Then the *post-interventional* distribution $P(Y = y | \text{do}(X = x))$, which involves the *do*-operator and is not the same as the conditional distribution, is used to assess whether and in what way X affects Y . As mentioned before, however, we assume a non-manipulable complex system and, therefore, study a weaker notion of causality. From observational data alone, causal effects can only be estimated (or *identified*) under certain assumptions about the underlying process and the kind of interventions [19, 63]. In Sect. VIA we discuss Pearl’s causal effect for linear models.

II. INFORMATION-THEORETIC PRELIMINARIES

A. Mutual information and conditional mutual information

Shannon’s entropy H [59, 60] is a measure of the uncertainty about outcomes of a process. *Mutual information* (MI),

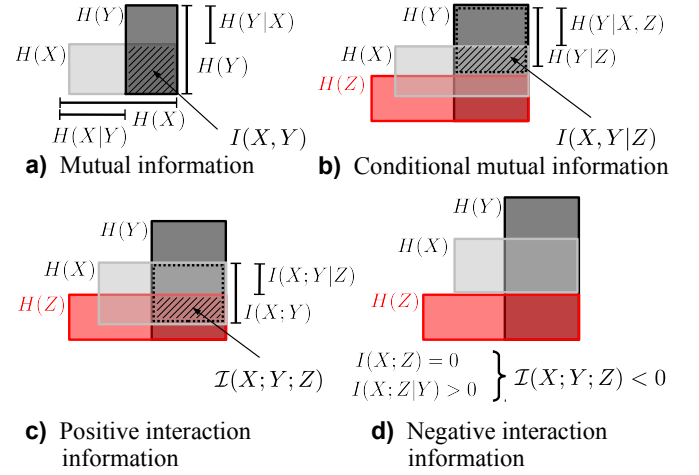


Figure 2. Venn diagrams of (conditional) mutual information and interaction information. The analogy between entropies and sets should not be overinterpreted since the interaction information can also be negative (for example, if the entropies of X and Z do not ‘overlap’ anymore as shown in (d)).

on the other hand, is a measure of the reduction of this uncertainty if another process is measured. The Shannon type MI between two real-valued (possibly multivariate) processes X and Y is defined as

$$I(X;Y) = \int \int p(x,y) \ln \frac{p(x,y)}{p(x)p(y)} dx dy \quad (2)$$

$$= H(Y) - H(Y|X) = H(X) - H(X|Y), \quad (3)$$

i.e., in the form of Eq. (3) as the difference between the uncertainty in Y and the remaining uncertainty if X is already known (and vice versa). Or in Eq. (2) as a certain Kullback-Leibler distance [4, 64] between the distributions $p(x,y)$ and the distribution for the independent case $p(x)p(y)$. From the definition it immediately follows that MI is symmetric in its arguments and zero if and only if X and Y are independent. Here we use the natural logarithm to measure MI and derived measures in *nats*. Further, using Jensen’s inequality [4] one can show that MI is always non-negative (which holds for the continuous as well as the discrete case).

The most important measure used throughout this article is the *conditional mutual information* (CMI) given by

$$I(X;Y|Z) = H(Y|Z) - H(Y|X,Z) = H(X|Z) - H(X|Y,Z) \quad (4)$$

$$= \int p(z) \iint p(x,y|z) \log \frac{p(x,y|z)}{p(x|z) \cdot p(y|z)} dx dy dz. \quad (5)$$

It can be phrased as the MI between X and Y that is not contained in a third variable Z . Just like MI, CMI is non-negative and symmetric in its first two arguments $I(X;Y|Z) = I(Y;X|Z)$. Further, according to Eq. (5) CMI

is zero if and only if X and Y are independent *conditionally on Z* ,

$$\begin{aligned} X \perp\!\!\!\perp Y|Z &\iff p(x, y|z) = p(x|z)p(y|z) \\ &\iff I(X; Y|Z) = 0. \end{aligned} \quad (6)$$

This property makes CMI especially useful to measure conditional independence as needed in the definition and estimation of causal graphs (Sect. III). Figures 2(a) and (b) visualize MI and CMI in Venn diagrams as a difference of conditional entropies. In this representation also the symmetry in the arguments is obvious.

B. Interaction information

Just as MI and CMI are differences of conditional entropies, also the difference of CMIs has an interesting interpretation that we will utilize to measure the effect of one random variable on the interaction between two others. Such a measure has been studied by [65–67] under the name *multiple information*. We use the term *interaction information* with the symbol \mathcal{I} , which is symmetrically defined as

$$\begin{aligned} \mathcal{I}(X; Y; Z) &= I(X; Y) - I(X; Y|Z) \\ &= I(Y; Z) - I(Y; Z|X) \\ &= I(Z; X) - I(Z; X|Y). \end{aligned} \quad (7)$$

In Refs. [68, 69] this quantity is defined with the signs reversed, but the above definition is more consistent with the definition of MI in Eq. (3), i.e., the conditional quantity is subtracted from the unconditional one. It is also straightforward to define the *conditional interaction information*

$$\mathcal{I}(X; Y; Z|W) = I(X; Y|W) - I(X; Y|Z, W). \quad (8)$$

Contrary to CMI, the (conditional) interaction information can also be negative and is bounded by

$$\begin{aligned} &-\min(I(X; Y|Z, W), I(Y; Z|X, W), I(Z; X|Y, W)) \\ &\leq \mathcal{I}(X; Y; Z|W) \\ &\leq \min(I(X; Y|W), I(Y; Z|W), I(Z; X|W)). \end{aligned} \quad (9)$$

The possible negativity also shows that the visualization in Fig. 2(c) as sets in Venn diagrams should not be overinterpreted. In Fig. 2(d) a case is shown where X and Z are *unconditionally* independent, but conditionally dependent leading to $I(X; Z|Y) \geq I(X; Z)$ and, therefore, a negative interaction information. That this property can actually be intuitively understood will be studied in examples in Sect. V.

C. Estimation of (conditional) mutual information

Instead of the commonly used binning estimators, here we use an advanced nearest-neighbor estimator [51, 70] that is

most suitable for variables taking on a continuous range of values. This estimator has as a free parameter the number of nearest-neighbors k which determines the size of hypercubes around each (high-dimensional) sample point. Small values of k lead to a lower estimation bias but higher variance and vice versa. For independence tests, a higher k with lower variance is more important while for estimates of the CMI value a smaller k is recommended. Note that for an estimation from (multivariate) time series stationarity is required.

III. TIME SERIES GRAPHS

A. Definition

A *time series graph* [46, 71] is a certain type of graphical model [45] for the case of time-ordered data and visualizes the Markovian conditional independence properties of a multivariate time-dependent process, i.e., how the joint density of the multivariate process \mathbf{X} (including its lags) factorizes. Figures 3 and 4(a) show examples. Each node in a time series graph represents a subprocess of a multivariate discrete time process \mathbf{X} at a certain time t . Directed links between subprocesses (or nodes) $X_{t-\tau}$ and Y_t for $\tau > 0$ are marked by an arrow and defined by

$$X_{t-\tau} \rightarrow Y_t \iff I(X_{t-\tau}; Y_t | \mathbf{X}_t^- \setminus \{X_{t-\tau}\}) > 0, \quad (10)$$

with infinite past $\mathbf{X}_t^- = (\mathbf{X}_{t-1}, \mathbf{X}_{t-2}, \dots)$, i.e., if they are not independent conditionally on the past of the whole process, which implies a lag-specific Granger causality with respect to \mathbf{X} . If $Y \neq X$ we say that the link $X_{t-\tau} \rightarrow Y_t$ represents a *coupling or cross-link at lag τ* , while for $Y = X$ it represents an *autodependency or auto-link at lag τ* .

Since often also contemporaneous associations are of interest, we also define links between X_t and Y_t as in previous works [39, 72] by

$$X_t - Y_t \iff I(X_t; Y_t | \mathbf{X}_{t+1}^- \setminus \{X_t, Y_t\}) > 0, \quad (11)$$

where also the contemporaneous present $\mathbf{X}_t \setminus \{X_t, Y_t\}$ is included in the condition. Note that stationarity implies that $X_{t-\tau} \rightarrow Y_t$ whenever $X_{t'-\tau} \rightarrow Y_{t'}$ for any t' and correspondingly for contemporaneous links. In Ref. [46] also another version of contemporaneous links is defined, marked by a dashed line:

$$X_t \text{ --- } Y_t \iff I(X_t; Y_t | \mathbf{X}_t^-) > 0. \quad (12)$$

In the case of a multivariate autoregressive process, the latter definition corresponds to non-zero entries in the covariance matrix of the innovations, while the former corresponds to non-zero entries in the *inverse* covariance matrix [46]. One problem with Definition (11) is that it can potentially cause spurious links if, e.g., X_t and Y_t are independent (also of the past), but both causally drive another process Z_t instantaneously, i.e., at the same time t , which might be due to a

too coarse time resolution interval. Then $I(X_t; Y_t) = 0$, but $I(X_t; Y_t | Z_t) > 0$ due to the ‘conditioning on a common child’ effect, see e.g. [47], which is shown in Fig. 2(d). In this work, we are not considering instantaneous causal effects, but to circumvent this problem in practice, one can consider contemporaneous effects only if both Definitions (12) and (11) are satisfied. Note that both definitions result in slight differences in the definition of open and blocked paths through contemporaneous links as discussed further below.

B. Causal paths

The measures introduced in Sect. IV are CMIs based on paths and different sets of conditions which we determine from the sets of parents and neighbors of a node Y_t defined, respectively, as

$$\mathcal{P}_{Y_t} = \{Z_{t-\tau} : Z \in \mathbf{X}, \tau > 0, Z_{t-\tau} \rightarrow Y_t\}, \quad (13)$$

$$\mathcal{N}_{Y_t} = \{X_t : X \in \mathbf{X}, X_t - Y_t\}. \quad (14)$$

Our main interest lies in *causal paths* in the time series graph which are defined as directed paths, i.e., containing only motifs $\rightarrow \bullet \rightarrow$ (assuming that the arrow of time in the time series graph goes to the right). But there are also other paths on which information is shared even though no causal interventions could ‘travel’ along these. In general [46], in the above defined time series graph with solid contemporaneous links a path between two nodes u and v is called *open* if it contains only the motifs $\rightarrow \bullet \rightarrow$, $\leftarrow \bullet \rightarrow$, $-\bullet \rightarrow$, or $-\bullet -$. On the other hand, if any motif on a path is $\rightarrow \bullet \leftarrow$ or $\rightarrow \bullet -$, the path is blocked. Nodes in such motifs are also called *colliders*. If we now consider a *separating or conditioning set* \mathcal{S} , openness and blockedness of conditioned motifs reverse, i.e., denoting a conditioned node by \blacksquare , the motifs $\rightarrow \blacksquare \rightarrow$, $\leftarrow \blacksquare \rightarrow$, $-\blacksquare \rightarrow$, and $-\blacksquare -$ are blocked and the motifs $\rightarrow \blacksquare \leftarrow$ and $\rightarrow \blacksquare -$ become open. Note that for the alternative definition of contemporaneous links Eq. (12) marked with dashed lines, the motif $--- \bullet ---$ is blocked while the conditioned motif $--- \blacksquare ---$ is open.

Two nodes u and v are *separated given a set* \mathcal{S} if all paths between the two are blocked. Conversely, two nodes are *connected given a set* \mathcal{S} if at least one path between the two is open. The Markov property, which we assume throughout, now relates separation in the time series graph to conditional independence relations in the underlying process which can be quantified with CMI (as a conditional independence relation):

$$u \text{ and } v \text{ separated given } \mathcal{S} \implies I(u; v | \mathcal{S}) = 0. \quad (15)$$

The path-based CMIs are constructed with conditions to block all non-causal paths and only leave open causal paths. In particular, also *contemporaneous sidepaths*, which start with one or more contemporaneous links followed by a directed path $u - \bullet - \dots - \bullet \rightarrow \dots \rightarrow v$, need to be blocked. Note that we do not consider contemporaneous causal effects here which might occur due to a too low sampling rate of the process.

C. Reconstruction

In Ref. [20] an algorithm for the estimation of the above-defined time series graphs by iteratively inferring the parents and, in a second step, also the neighbors was introduced. This algorithm is a modification of the PC algorithm [18, 48] for time series graphs. The main idea is to iteratively unveil the links from parents and contemporaneous neighbors by testing for conditional independence between all possible pairs of nodes conditioned on iteratively more conditions and testing all combinations among them. Due to the careful, step-wise conditioning, the dimension stays as low as possible in every iteration step. This important feature helps to alleviate the curse of dimensionality in estimating CMIs. Due to a smart handling of the choice of conditions, the combinatorial explosion is also efficiently avoided in most practical cases leading to a polynomial dependence on the number of variables [48]. The complexity can also be controlled by limiting certain parameters like the conditioning dimension. See [73] for an analysis of computational complexity where we also partially investigate the computational complexity of forward-selection based approaches [41, 42]. Forward selection, as used in Refs. [14, 15, 36, 41–44], iteratively selects variables based on how much information they contain *additionally* to the already chosen variables using CMI. This increases the estimation dimension in every step making conditional independence tests more unreliable. Note that, as shown in Appendix A, a forward selection alone cannot be used to reconstruct causal drivers because spurious drivers can be selected. The necessary backward elimination step also involves a very high dimensional independence test.

The causal algorithm introduced in Ref. [20] avoids high-dimensionality by making certain assumptions. In particular, the consistency of the PC algorithm has been proven under the assumption of the *Causal Markov Condition*, i.e., that separation implies conditional independence (Eq. (15)), and *Faithfulness* [18] which guarantees that the graph entails all conditional independence relations true for the underlying process. One pathological example of unfaithfulness is a true graph with links $X \rightarrow Y \rightarrow Z$ with another direct link $X \rightarrow Z$ with a counteracting contribution to the total effect of X on Z that fully balances out the indirect contribution leading to a zero net causal effect. Then X is independent of Z and the causal discovery algorithm would remove the link between X and Z already in the first step. Although a counteracting mechanism need not always fully erase another mechanism, finite sample effects can pose a problem [74]. While this calls for modifications of the algorithm in these situations, it does not affect the definition of causal links in Eq. (10). Also for an exclusively *synergistic* causal driving, e.g., the XOR-gate [57], faithfulness is violated. Such cases can often only be recovered if all possible subsets of variables are tested, while the PC-algorithm makes the above Faithfulness assumption to overcome the explosion of computational complexity. Which CMI-based algorithm is best for a given application regarding their underlying assumptions, statistical power, consistency, and computational complexity is still an open research question.

In practice, the significance level or fixed threshold used in the independence tests of the causal algorithm is not a very reliable indicator for the final significance level of causal links because links are tested sequentially and, therefore, Bonferroni corrections cannot be easily applied. To overcome this problem, a different approach consisting of two steps is recommended: (i) Inferring the parents and neighbors of each component with the causal algorithm, and (ii) testing the significance of each possible link again using the multivariate momentary information transfer [39] discussed below with an appropriate shuffle test or a fixed threshold. This is beneficial because MIT alleviates the influence of strong autodependencies on independence tests. Nevertheless, each significance level or fixed threshold in the causal algorithm as well as the subsequent MIT independence test will result in a different time series graph. Since the causal pathway analysis depends sensitively on the existence of links in the graph, in practice the whole pathway analysis introduced in the following can be studied for different significance levels or fixed thresholds of the causal reconstruction.

IV. TIME SERIES GRAPH BASED MEASURES OF INFORMATION TRANSFER (TIGRAMITE APPROACH)

In the following we discuss well-known and novel measures to quantify different aspects of information transfer through causal links and paths. As mentioned in the introduction, the proposed measures of information transfer are CMIs based on different sets of conditions which we determine from the reconstructed time series graph. This framework is called the *Tigramite* approach. This approach has the advantage of a low-dimensional estimation problem without arbitrary truncation parameters like in the original definition of transfer entropy involving infinite vectors.

A. Lagged mutual information

The first and simplest association measure combining information theory with time series is the lagged (cross-)mutual information given by

$$I_{XY}^{\text{MI}}(\tau) = I(X_{t-\tau}; Y_t). \quad (16)$$

For $\tau > 0$, MI measures the information in the past of X that is contained in Y . MI is not intended to exclude entropy common to both $X_{t-\tau}$ and Y_t , yet it is frequently used to determine the time delay of an interaction mechanism, admitting that there does not necessarily exist a causal relation. The ambiguity in interpreting the value of MI is discussed in Ref. [39] and the problem that coupling delays cannot be properly inferred with MI because the peak of the lag function is shifted for strong autocorrelations is analyzed in Ref. [50] for the analogous problem with the lagged correlation function.

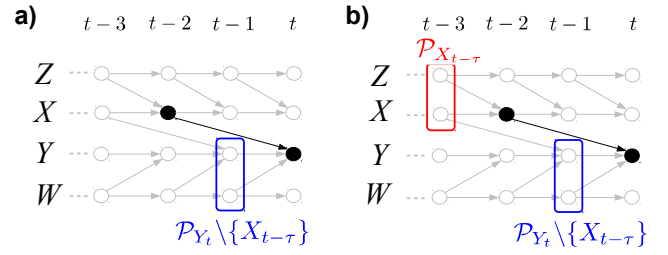


Figure 3. Time series graphs (see definition in Sect. III) illustrating the causal link-based multivariate ITY (a), and MIT (b). The respective CMIs are between $X_{t-\tau}$ and Y_t (marked by the black dots) conditioned on the sets marked by the colored boxes.

B. Information transfer and transfer entropy

The weaknesses of MI as a measure of information transfer have been discussed early on, most notably by Schreiber [32]. The key point to arrive at a causal notion of information transfer is to exclude information from common drivers shared by X and Y . Implementing this idea, Schreiber introduced *transfer entropy* (TE) [32] which is the information-theoretic analogue of Granger causality and for multivariate Gaussian processes they can actually be shown to be equivalent [75]. In the original article TE is defined between two variables and is not lag-specific. Here we will focus on a more general multivariate and lag-specific variant of TE introduced in Ref. [39], the *information transfer to Y* (ITY)

$$I_{X \rightarrow Y}^{\text{ITY}}(\tau) = I(X_{t-\tau}; Y_t | \mathcal{P}_{Y_t} \setminus \{X_{t-\tau}\}) \quad (17)$$

$$= H(Y_t | \mathcal{P}_{Y_t} \setminus \{X_{t-\tau}\}) - H(Y_t | \mathcal{P}_{Y_t}), \quad (18)$$

where the latter term is the source entropy of Y . ITY is different from a bivariate lag-specific TE definition such as in Ref. [34] discussed in the introduction since it explicitly uses the previously reconstructed parents $\mathcal{P}_{Y_t} \subset \mathbf{X}^-$, which includes drivers from the past of the whole process and not only Y 's own past. Due to this condition, ITY is non-zero only for directly causally linked nodes in the time series graph. Figure 3(a) shows an example time series graph to illustrate the multivariate ITY. In analogy, one can also define a contemporaneous ITY [76]. Note that ITY or the multivariate TE are zero for indirectly causal interactions and will not be further discussed here.

C. Momentary information transfer

ITY is non-zero only for causal links, but its value does not fulfill the property of coupling strength autonomy [39] implying that its interpretation is quite ambiguous, e.g., in the presence of autocorrelations. The central idea of *momentary information transfer* (MIT) is to provide a better interpretability for the strength of causal links. MIT between X at some lagged time $t - \tau$ in the past (i.e., $\tau > 0$) and Y at time t is the

CMI that measures the part of the entropy of Y that is shared with the source entropy of X (see Sect. I C) relative to the entropy that excludes information from *both* parents (Fig. 3(b)):

$$\begin{aligned} I_{X \rightarrow Y}^{\text{MIT}}(\tau) &= I(X_{t-\tau}; Y_t | \mathcal{P}_{Y_t} \setminus \{X_{t-\tau}\}, \mathcal{P}_{X_{t-\tau}}) \\ &= H(Y_t | \mathcal{P}_{Y_t} \setminus \{X_{t-\tau}\}, \mathcal{P}_{X_{t-\tau}}) - H(Y_t | \mathcal{P}_{Y_t}), \end{aligned} \quad (19)$$

where the condition in the last term can be reduced since $H(Y_t | \mathcal{P}_{Y_t}, \mathcal{P}_{X_{t-\tau}}) = H(Y_t | \mathcal{P}_{Y_t})$ because $\mathcal{P}_{X_{t-\tau}}$ is independent of Y_t given \mathcal{P}_{Y_t} (if the sets overlap, common conditions are included only in \mathcal{P}_{Y_t}). The attribute *momentary* [38] is used because MIT measures the information of the “moment” $t - \tau$ in X that is transferred to Y_t . Because MIT uses the parents \mathcal{P}_{Y_t} as conditions, just like ITY it is non-zero only for causal links in the time series graph. Further, as shown in Sect. V C, the additional condition on the parents $\mathcal{P}_{X_{t-\tau}}$ makes it fulfill the property of coupling strength autonomy. Similarly to the definition of contemporaneous links in Eq. (11), one can also define a contemporaneous MIT [39].

Note that in the original article introducing the idea of momentary information transfer, Ref. [38], a *bivariate MIT* was defined as

$$I_{X \rightarrow Y}^{\text{bivMIT}}(\tau) = I(X_{t-\tau}; Y_t | Y_t^-, X_{t-\tau}^-), \quad (20)$$

i.e., including only the past of both processes as a condition. This bivariate MIT was used not only to quantify causal strength, but also to detect causal links and delays by looking for peaks in the lagged bivariate MIT-function. This approach fails, however, in certain cases [34, 40] and cannot be generally recommended. Rather, as mentioned before, the iterative causal reconstruction should also be used for bivariate applications. Then the multivariate MIT and related measures can be studied on the basis of the inferred time series graph (Tigramite approach).

Each of the CMIs introduced in the preceding sections are intended to measure a different aspect of the causal coupling link between X and Y at some lag τ . In the analytical analysis of simple models (Sect. V) we will briefly review the interpretability of the different measures, for a detailed account see [39].

D. Quantifying information transfer along paths

In this article the main question of interest is not only how strong a causal link is, but more generally how strong an indirect causal influence of a variable $X_{t-\tau}$ on Y_t is (Fig. 4). Indirect causal effects can only be transferred on *causal paths* in the time series graph, which are paths consisting only of directed links as defined in Sect. III B. Note that Fig. 4(b) shows an aggregated process graph, which is not suited to read off causal paths since it does not show autodependencies like time series graphs.

We denote the processes along causal paths including $X_{t-\tau}$ for $\tau > 0$ and excluding Y_t by

$$\begin{aligned} \mathcal{C}_{X_{t-\tau} \rightarrow Y_t} &= \{X_{t-\tau}\} \cup \\ &\quad \{W_{t-\tau_W} \in \mathbf{X}_t^- \text{ with } \tau > \tau_W > 0 : \\ &\quad X_{t-\tau} \rightarrow \dots \rightarrow W_{t-\tau_W} \rightarrow \dots \rightarrow Y_t\}, \end{aligned} \quad (21)$$

where $\rightarrow \dots \rightarrow$ denotes a succession of directed links or only one directed link. These can be read off directly from the time series graph. For example, in Fig. 4, X_{t-3} and Y_t are connected by the three causal paths $X_{t-3} \rightarrow W_{2,t-1} \rightarrow Y_t$, $X_{t-3} \rightarrow W_{1,t-2} \rightarrow Y_t$, and $X_{t-3} \rightarrow W_{1,t-2} \rightarrow W_{2,t-1} \rightarrow Y_t$ such that $\mathcal{C}_{X_{t-3} \rightarrow Y_t} = \{X_{t-3}, W_{1,t-2}, W_{2,t-1}\}$. Our goal is now to construct a CMI with conditions that leave open only these causal paths and block all non-causal paths according to the definition of paths and blocking in time series graphs in Sect. III B.

The first step is to exclude paths due to common drivers of X and Y . The parents $\mathcal{P}_{X_{t-\tau}}$ of X at time $t - \tau$ block all common drivers from the past since these paths necessarily contain the motifs $-\bullet \rightarrow X_{t-\tau}$ or $\rightarrow \bullet \rightarrow X_{t-\tau}$, which are both blocked if conditioned on. A second class of non-causal paths are contemporaneous sidepaths as defined in Sect. III B. These can be blocked by conditioning on those contemporaneous neighbors of $X_{t-\tau}$ that have at least one contemporaneous sidepath, of course *not traversing* $X_{t-\tau}$, which we define as

$$\mathcal{N}_{X_{t-\tau}}^{Y_t} = \{W_{t-\tau} \in \mathcal{N}_{X_{t-\tau}} : X_{t-\tau} - W_{t-\tau} \overset{\rightarrow}{\dots} \rightarrow Y_t\}, \quad (22)$$

where $\overset{\rightarrow}{\dots} \rightarrow$ denotes a contemporaneous sidepath that does not involve $X_{t-\tau}$. For example, in Fig. 4(a), $\mathcal{N}_{X_{t-3}}^{Y_t} = \{W_{1,t-3}\}$, but for the autodependency $X_t \rightarrow X_{t-1}$ we have $\mathcal{N}_{X_{t-1}}^{X_t} = \emptyset$, since there are no contemporaneous sidepaths from $W_{1,t-1}$ to X_t . The condition on neighbors unfortunately introduces new open paths because $X_{t-\tau} - \blacksquare \leftarrow$ is an open motif. To block these paths, one needs to additionally condition on the parents of the neighbors $\mathcal{P}(\mathcal{N}_{X_{t-\tau}}^{Y_t})$. Note that one could also only select those parents from $X_{t-\tau}$ which have a ‘common driver path’ to Y_t , but our goal is to isolate the momentary information *entering the system in* X , i.e., the dynamical noise from model (1), and quantify its propagation along causal paths to Y some time later. The *information transfer from* X (ITX) is now defined for $\tau > 0$ as

$$I_{X_{t-\tau} \rightarrow Y_t}^{\text{ITX}} = I(X_{t-\tau}; Y_t | \mathcal{P}_{X_{t-\tau}}, \mathcal{N}_{X_{t-\tau}}^{Y_t}, \mathcal{P}(\mathcal{N}_{X_{t-\tau}}^{Y_t})). \quad (23)$$

It measures the part of source entropy in $X_{t-\tau}$ that reaches Y_t on any causal path and could be regarded as an information-theoretic quantification of Sims causality as mentioned in the introduction. In Ref. [39] this measure was introduced without the condition on neighbors.

ITX does not exclude information entering process Y_t from other sources, for example from process Z_3 in the example shown in Fig. 4. The idea of momentary information transfer was to isolate the information shared between two processes

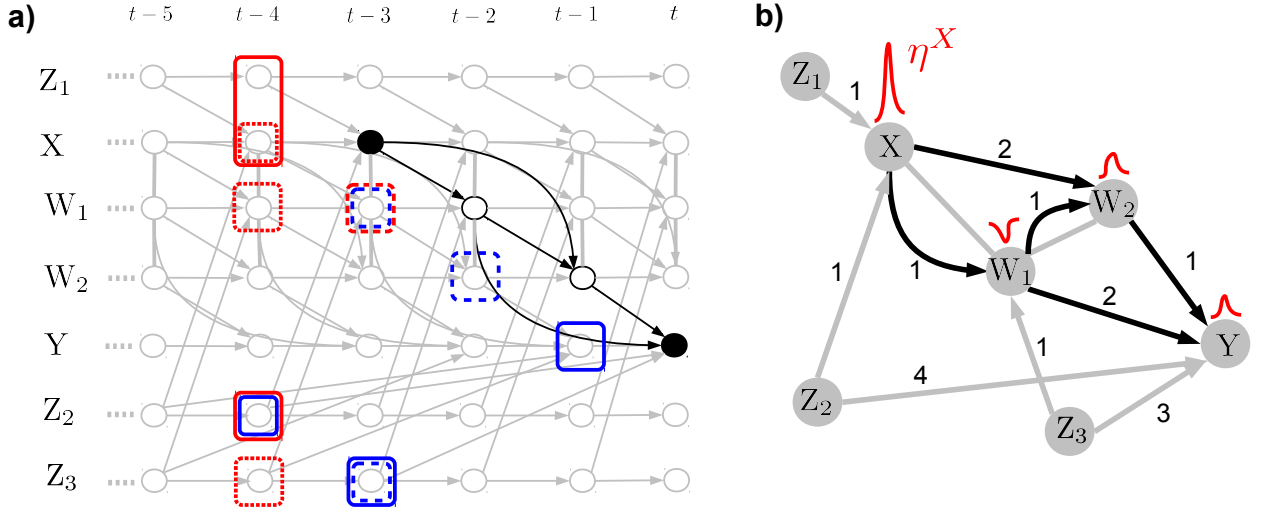


Figure 4. (a) Time series graph and (b) process graph illustrating path-based measures of information transfer and interaction (the labels denote the lags). Directed links (Def. 10) are marked by arrows, contemporaneous links (Def. 11) by a solid line. There are three causal directed paths connecting X_{t-3} and Y_t (black lines), two of length 2 via $W_{1,t-2}$ and $W_{2,t-1}$ and one of length 3: $X_{t-3} \rightarrow W_{1,t-2} \rightarrow W_{2,t-1} \rightarrow Y_t$. The idea of the measure ITX here is to quantify how much of the information entering the system in X_{t-3} , i.e., the dynamical noise η^X , is transferred along causal paths to Y_t by conditioning out the effect of the parents of $\mathcal{P}_{X_{t-3}}$ (solid red boxes), its neighbors involving contemporaneous sidepaths to Y_t denoted $\mathcal{N}_{X_{t-3}}^{Y_t}$ (dashed red boxes), and the neighbor's parents $\mathcal{P}(\mathcal{N}_{X_{t-3}}^{Y_t})$ (dotted red boxes). The latter two conditioning sets exclude contemporaneous sidepaths like $X_{t-3} - W_{1,t-3} \rightarrow W_{1,t-2} \rightarrow W_{2,t-1} \rightarrow Y_t$. ITX is still influenced by processes affecting intermediate nodes on causal paths, e.g., process Z_3 which drives W_1 and Y . The idea of MITP now is to go one step further and isolate all causal paths from the remaining process by additionally conditioning on the parents of the intermediate path nodes $\mathcal{C}_{X_{t-\tau} \rightarrow Y_t} \setminus \{X_{t-\tau}\}$ (dashed blue boxes) and Y (solid blue boxes). This also allows to isolate mediated effects using momentary interaction information as defined in Sect. IV E.

via a causal link from the remaining process. Now this idea can be generalized by isolating all causal (directed) paths from the remaining process to assess the part of the source entropy of $X_{t-\tau}$ that is transferred on any causal path and shared with Y_t , excluding the parents of all intermediate path nodes and Y that are not part of the causal path. Figure 4 illustrates this idea. With the nodes on all causal paths including $X_{t-\tau}$ denoted by $\mathcal{C}_{X_{t-\tau} \rightarrow Y_t}$ (Eq. (21)), the *momentary information transfer along causal paths* (MITP) is defined as

$$I_{X \rightarrow Y}^{\text{MITP}}(\tau) = I(X_{t-\tau}; Y_t | \mathcal{P}_{Y_t} \setminus \mathcal{C}_{X_{t-\tau} \rightarrow Y_t}, \mathcal{P}(\mathcal{C}_{X_{t-\tau} \rightarrow Y_t}), \mathcal{N}_{X_{t-\tau}}^{Y_t}, \mathcal{P}(\mathcal{N}_{X_{t-\tau}}^{Y_t})). \quad (24)$$

For the time series graph example in Fig. 4, these conditions are marked by the red and blue boxes. In Sect. V we will prove that MITP, contrary to ITX, also fulfills a generalized coupling strength autonomy theorem which allows to better relate it to the underlying dynamics of a process as will be discussed in Sect. VI. If $\mathcal{C}_{X_{t-\tau} \rightarrow Y_t} = \{X_{t-\tau}\}$, and under the “no sidepath”-constraint in Ref. [39], the conditions on the neighbors can be dropped and MITP collapses to MIT.

E. Quantifying mediating information transfer

Looking at Fig. 4, one immediate question is whether one can quantify how much of the information transfer between X and Y went through W_1 and how much through W_2 ? Which of these is information-theoretically more important for explaining the indirect causal relationship between X and Y ? The interaction information defined in Eq. (7) can be used to answer this question, we here discuss two analogous versions for the measures ITX and MITP. For two processes $X_{t-\tau}$ and Y_t connected by a causal path, intermediate processes can occur with multiple lags. For example, among the causal paths between X_{t-4} and Y_t in Fig. 4, the process W_1 is traversed at lags $W_{1,t-2}$ and $W_{1,t-3}$. Generally, if a subprocess W is intermediate in an interaction $X_{t-\tau} \rightarrow \dots \rightarrow Y_t$ at multiple lags $t - \tau_1, t - \tau_2, \dots$, we here include all these lags in the vector $\mathbf{W} = \{W_{t-\tau_1}, W_{t-\tau_2}, \dots\} \subset \mathcal{C}_{X_{t-\tau} \rightarrow Y_t}$.

First, we define the *interaction information from X* (IIX) as

$$\mathcal{I}_{X_{t-\tau} \rightarrow Y_t | \mathbf{W}}^{\text{IIX}} = I(X_{t-\tau}; Y_t; \mathbf{W} | \mathcal{P}_{X_{t-\tau}}, \mathcal{N}_{X_{t-\tau}}^{Y_t}, \mathcal{P}(\mathcal{N}_{X_{t-\tau}}^{Y_t})) \quad (25)$$

$$= I_{X \rightarrow Y}^{\text{ITX}}(\tau) - \underbrace{I(X_{t-\tau}; Y_t | \mathcal{P}_{X_{t-\tau}}, \mathcal{N}_{X_{t-\tau}}^{Y_t}, \mathcal{P}(\mathcal{N}_{X_{t-\tau}}^{Y_t}), \mathbf{W})}_{\text{ITX conditioned on } \mathbf{W}}. \quad (26)$$

IIX measures the effect of an intermediate process \mathbf{W} on the information transfer between the source information of $X_{t-\tau}$ and Y_t . Second, the *momentary interaction information* (MII) for an intermediate process \mathbf{W} is defined as

$$\begin{aligned} \mathcal{I}_{X \rightarrow Y|\mathbf{W}}^{\text{MII}}(\tau) &= \mathcal{I}(X_{t-\tau}; Y_t; \mathbf{W} \mid \mathcal{P}_{Y_t} \setminus \mathcal{C}_{X_{t-\tau} \rightarrow Y_t}, \mathcal{P}(\mathcal{C}_{X_{t-\tau} \rightarrow Y_t}), \\ &\quad \mathcal{N}_{X_{t-\tau}}^{Y_t}, \mathcal{P}(\mathcal{N}_{X_{t-\tau}}^{Y_t})) \quad (27) \\ &= \underbrace{I_{X \rightarrow Y}^{\text{MITP}}(\tau) - I(X_{t-\tau}; Y_t \mid \mathcal{P}_{Y_t} \setminus \mathcal{C}_{X_{t-\tau} \rightarrow Y_t}, \mathcal{P}(\mathcal{C}_{X_{t-\tau} \rightarrow Y_t}), \\ &\quad \mathcal{N}_{X_{t-\tau}}^{Y_t}, \mathcal{P}(\mathcal{N}_{X_{t-\tau}}^{Y_t}), \mathbf{W})}_{\text{MITP conditioned on } \mathbf{W}}. \quad (28) \end{aligned}$$

MII measures the effect of \mathbf{W} on the momentary information transfer along paths between $X_{t-\tau}$ and Y_t and additionally isolates the influence of drivers of the causal path processes. In Section V we discuss several examples demonstrating that IIX and MII are not necessarily always positive implying that an intermediate process can counteract the interaction between $X_{t-\tau}$ and Y_t . This measure can naturally be extended by including sets of processes from $\mathcal{C}_{X_{t-\tau} \rightarrow Y_t}$. Due to the symmetry of interaction information as defined in Eq. (7), MII is symmetric in its arguments excluding the condition.

In a climate data example in Sect. VII, we will see how IIX and MII can be used to quantify dominant pathway mechanisms and in Sect. VI C we discuss how they can be used as an aggregate measure of ‘causal interaction betweenness’, modifying concepts from complex network theory for functional network analysis [1].

V. EXAMPLES AND THEOREMS

A. Linear model example

In Ref. [39] the strength of direct causal links was studied. The main finding was that MIT solely depends on the coefficient corresponding to the causal link. This property was called *coupling strength autonomy* in Ref. [39] and will be reviewed in Sect. V C. For the case of interactions along causal paths, consider the following linear model with time series graph visualized in Fig. 5(a):

$$\begin{aligned} X_t &= \alpha X_{t-1} + \eta_t^X \\ W_t &= \alpha W_{t-1} + a X_{t-1} + \eta_t^W \\ Y_t &= \alpha Y_{t-1} + c X_{t-2} + b W_{t-1} + \eta_t^Y, \quad (29) \end{aligned}$$

where all processes are jointly zero-mean Gaussian with variances $\sigma_X^2, \sigma_Y^2, \sigma_Z^2$ of the innovation terms η . Here the influence of X_{t-2} on Y_t has two paths: One via the direct coupling link $X_{t-2} \rightarrow Y_t$ and one via the path $X_{t-2} \rightarrow W_{t-1} \rightarrow Y_t$ such that we can rewrite

$$Y_t = c X_{t-2} + b(a X_{t-2} + \eta_{t-1}^W) + \eta_t^Y, \quad (30)$$

from which we see that the coupling cannot be unambiguously related to one coefficient and interesting dynamics emerge. In Fig. 5(b) we investigate the measures ITX, MITP, IIX, and MII numerically for varying $a = b$ (strength of the sidepath) and c (strength of direct link) for fixed autodependency strength $\alpha = 0.5$. We assume $a, b \neq 0$, because otherwise this causal path vanishes and IIX or MII are not defined. The ensemble size to estimate the ensemble mean is 30, the sample length is $T = 10,000$, and the CMI nearest-neighbor estimation parameter is $k = 1$ [52] to achieve minimal bias. As mentioned in Sect. II C, for larger k the bias increases, but also the estimator’s variance decreases [52] making higher k values a better choice for independence tests as used in the causal algorithm.

Since we vary a together with b , the contribution via this sidepath is always positive, also for negative a, b . If also c is positive, we observe an increase in ITX as well as MITP (Fig. 5(b)), with the latter being more pronounced. For negative c , on the other hand, the contributions of the direct link and the sidepath *counteract* and, for certain values (a, b, c) even cancel out leading to a vanishing ITX and MITP.

These different types of mediation of the intermediate process W can be quantified by IIX and MII (lower panels in Fig. 5(b)): For positive c , both are larger than zero, showing the positive contribution of both mechanisms, also here MII is more pronounced. For $c = 0$, MII is equal to MITP because the only interaction stems from the causal path demonstrating the explanatory influence of W , which acts as the only mediating process. In the Venn diagram of Fig. 2(c) this corresponds to the case in which $H(W)$ entails all of the shared entropy between X and Y . For negative c , the counteracting effect is evident in the negative sign of IIX and MII which implies for the latter that $I_{X \rightarrow Y|\mathbf{W}}^{\text{MII}}(\tau = 2) > I_{X \rightarrow Y}^{\text{MITP}}(\tau = 2)$: Conditioning out the effect of the intermediate process W here reveals that the direct link is actually very strong and was only ‘masked’ by the counteracting sidepath via W .

In Fig. 5(c) the dependence of the four measures for $a = b = 0.5$ and varying the autodependency strength α and direct link strength c is shown. ITX features a strong dependency on α already for weak drivings $\alpha \approx 0.4$ and almost vanishes for a very strong driving. Note that the same effect would be observed if other external processes drive W and Y (from X the effect is partially excluded due to the condition on \mathcal{P}_X). Analytically, here ITX can only be reduced to

$$\begin{aligned} I_{X \rightarrow Y}^{\text{ITX}}(\tau = 2) &= I(X_{t-2}; Y_t | X_{t-3}) \\ &= I(\alpha X_{t-3} + \eta_{t-2}^X; Y_t | X_{t-3}) \\ &\stackrel{\text{Eq. (B6) in Appendix}}{=} I(\eta_{t-2}^X; Y_t | X_{t-3}), \quad (31) \end{aligned}$$

which still depends on many coefficients in the model and cannot be easily related to the underlying dynamics. On the other hand, MITP can be simply related to the coefficients along the causal paths as

$$I_{X \rightarrow Y}^{\text{MITP}}(\tau = 2) = \frac{1}{2} \ln \left(1 + \frac{(c + ab)^2 \sigma_X^2}{b^2 \sigma_W^2 + \sigma_Y^2} \right), \quad (32)$$

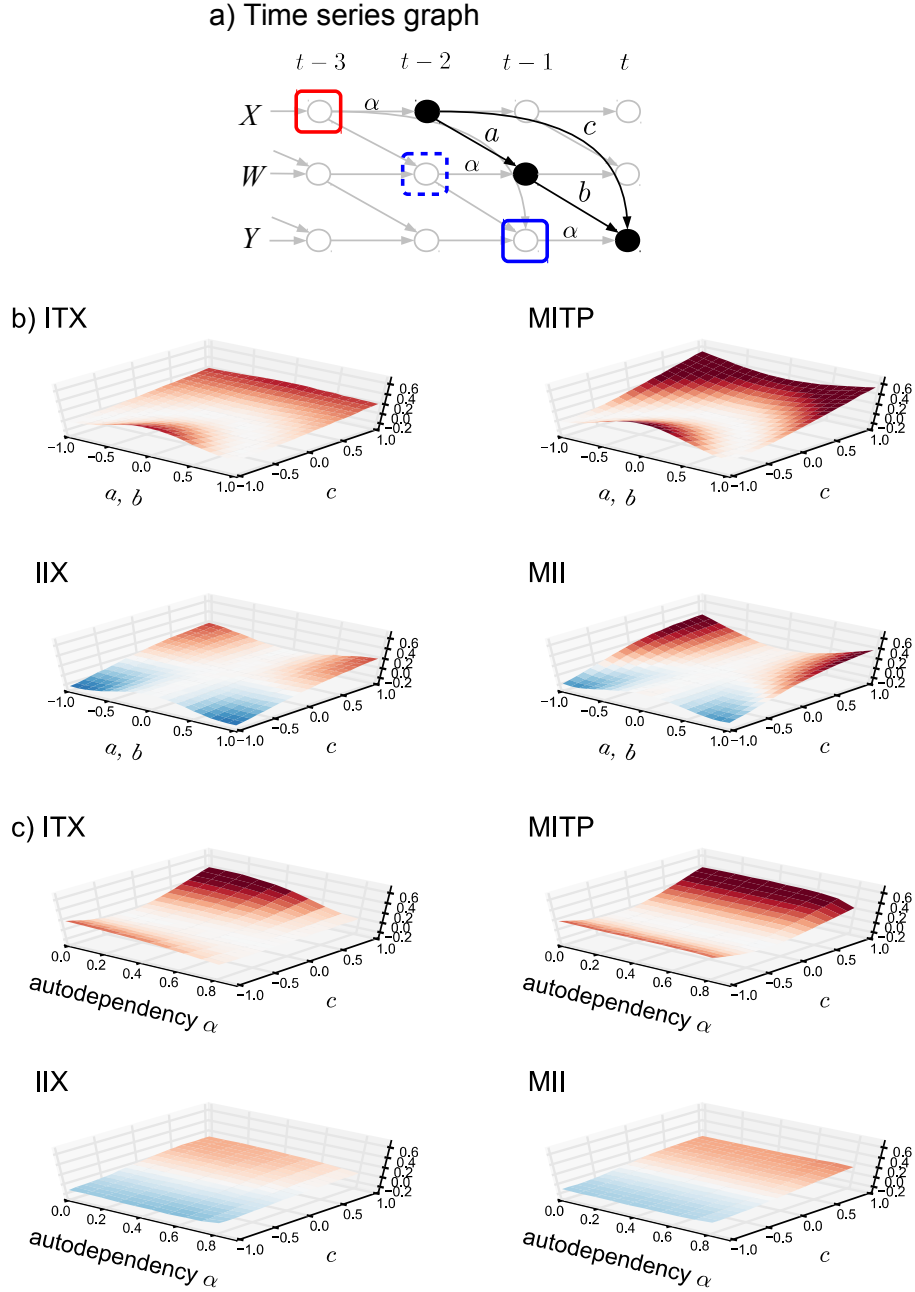


Figure 5. (a) Time series graph for model (29) of a causal interaction between three processes (black dots). The parents are shown in colored boxes, here there are no neighbors. a , b , c , α denote the model coefficients. In (b) the interaction measures are plotted against $a = b$ (strength of the sidepath) and c (strength of direct link) for an autodependency strength $\alpha = 0.5$, and in (c) against c and the autodependency strength α for $a = b = 0.5$. All innovation terms η have unit variance. Further parameters: ensemble size 30, sample length $T = 10,000$, nearest-neighbor estimation parameter $k = 1$.

which follows from Theorem 2 in Sect. V C. Here it becomes evident that MITP vanishes along the parabola $c = -ab$ (which can be considered a pathological case where the causal assumption of *faithfulness* is violated [18] as discussed in Sect. III). A second important finding is that MITP is *independent* of the autodependency coefficient α . The same holds for MII, here given by

$$\mathcal{I}_{X \rightarrow Y|W}^{\text{MII}} = \frac{1}{2} \ln \left(1 + \frac{(c + ab)^2 \sigma_X^2}{b^2 \sigma_W^2 + \sigma_Y^2} \right) - \frac{1}{2} \ln \left(1 + \frac{c^2 \sigma_X^2 \sigma_W^2}{(\sigma_W^2 + a^2 \sigma_X^2) \sigma_Y^2} \right), \quad (33)$$

as follows from Appendix B 4. This implies that the value of MITP and MII can solely be related to the model's coefficients along the causal interaction paths, which can be considered an advantage in interpreting these measures compared to ITX or IIX. While in this example there are no external parents influencing the processes along the path, in more complex schemes also their effect can be excluded by the condition on the parents of the nodes on the path denoted by $\mathcal{C}_{X_{t-\tau} \rightarrow Y_t}$. In Sect. 3 this will be proven for the general case. Note that in Fig. 5(c) MITP and MII are slightly affected for very strong autodependencies which is due to an estimation bias and vanishes for infinite sample sizes. This model will be further discussed in relation to linear causal effect measures in Sect. VIA.

B. Nonlinear model example

Next, we discuss a nonlinear version of model (29) which shares the same time series graph, but features different dynamics:

$$\begin{aligned} X_t &= \alpha X_{t-1} + \eta_t^X \\ W_t &= \alpha W_{t-1} + a X_{t-1} + \eta_t^W \\ Y_t &= \alpha Y_{t-1} + \underbrace{c b X_{t-2} W_{t-1}}_{\text{multiplicative dependency}} + \eta_t^Y, \end{aligned} \quad (34)$$

with Gaussian innovation terms as before. Figure 6(a) shows that ITX and MITP vanish for b or c equal zero and are increasing for larger absolute values. For larger $|c|$ and $a, b \approx \pm 0.5$ we observe a counteracting of W through the indirect path as can be seen from the negative IIX and MII, but no annihilation of both effects occurs here and ITX and MITP stay positive. For this nonlinear dependency structure both ITX and MITP (and the corresponding interaction informations) depend on the external forcing parameter α (Fig. 6(b)). The reason is that the nonlinearity mixes the terms and the dependencies cannot be conditioned out anymore. Consider model (34), but with differing autodependency terms α, β, γ for X, W, Y , respectively. MITP here is given by

$$\begin{aligned} I_{X \rightarrow Y}^{\text{MITP}}(\tau = 2) &= I(X_{t-2}; Y_t | X_{t-3}, W_{t-2}, Y_{t-1}) \\ &= I(\eta_{t-2}^X; Y_t | X_{t-3}, W_{t-2}, Y_{t-1}), \end{aligned} \quad (35)$$

and the dependency of Y_t can be rewritten as

$$\begin{aligned} Y_t &= cb(a\eta_{t-2}^X + \eta_{t-1}^W)\eta_{t-2}^X + \eta_t^Y \\ &\quad + cb(\alpha a X_{t-3}\eta_{t-2}^X + \alpha X_{t-3}\eta_{t-1}^W \\ &\quad + \beta W_{t-2}\eta_{t-2}^X + \alpha a X_{t-3}\eta_{t-2}^X) \\ &\quad + \gamma Y_{t-1} + cb(\alpha \beta X_{t-3}W_{t-2} + a\alpha^2 X_{t-3}^2). \end{aligned} \quad (36)$$

Here in MITP the last line vanishes due to the condition on $(X_{t-3}, W_{t-2}, Y_{t-1})$, but due to the multiplicative mixing in the second and third line, the autodependency coefficients

α, β (but not γ) still determine MITP. ITX additionally depends on γ . This model, therefore, demonstrates a case where 'external effects' cannot be excluded anymore. Thus, while the information-theoretic interpretation still holds, MITP cannot be easily related to the system's dynamics. Still, plots like in Figs. 5, 6 can help to better understand dynamical interactions also in toy models from nonlinear dynamics. In the next section we prove under which general assumptions the coupling strength autonomy holds for MITP and MII. The multiplicative dependency can be seen as an example of synergy which has recently gained a lot of interest in information-theoretical studies, see e.g. Refs. [77, 78]. In Ref. [73] synergistic effects are studied with respect to optimal prediction schemes.

C. Theorems

In this section we state some inequality relations among the novel measures and generalize the coupling strength autonomy theorem for MIT [39] to the path-based measures MITP and MII.

Theorem 1 (Inequality relations). *For $\tau > 0$, the following inequalities hold:*

$$I_{X \rightarrow Y | \mathbf{W}}^{\text{IIX}}(\tau) \leq I_{X \rightarrow Y}^{\text{ITX}}(\tau) \quad (37)$$

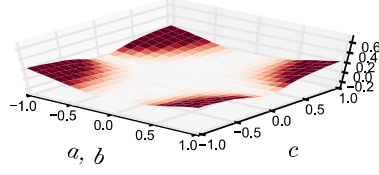
$$I_{X \rightarrow Y | \mathbf{W}}^{\text{MII}}(\tau) \leq I_{X \rightarrow Y}^{\text{MITP}}(\tau) \quad (38)$$

$$I_{X \rightarrow Y}^{\text{ITX}}(\tau) \leq I_{X \rightarrow Y}^{\text{MITP}}(\tau). \quad (39)$$

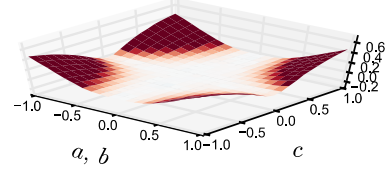
The first two inequalities are trivially fulfilled since IIX and MII are defined by ITX and MITP *minus* a CMI, which is always positive. Equality holds if the intermediate node(s) \mathbf{W} explain the entire interaction between X and Y . The last inequality is proven in appendix B 1. In practice, this inequality is often not fulfilled because the estimation dimension of MITP is typically much larger than that of ITX and finite sample effects lead to a negative bias which often leads to MITP being smaller than ITX. This also makes a comparison of the values of ITX and MITP more difficult.

To generalize the coupling strength autonomy theorem from MIT to MITP and MII, we consider causal paths as defined in Sect. III B instead of only causal links, thus, including also directed causal sidepaths which were excluded for MIT. While the careful condition on only those neighbors that have sidepaths excludes dependencies of MITP and MII on the dynamics along these sidepaths, one cannot avoid a contemporaneous dependency on the interaction with the respective neighbor itself. This also holds for other intermediate processes on causal paths. To prove the following theorems, we need the "no contemporaneous dependency"-condition. Denoting by $\mathcal{S}^{\text{MITP}} = (\mathcal{P}_{Y_t} \setminus \mathcal{C}_{X_{t-\tau} \rightarrow Y_t}, \mathcal{P}(\mathcal{C}_{X_{t-\tau} \rightarrow Y_t}), \mathcal{N}_{X_{t-\tau}}^{Y_t}, \mathcal{P}(\mathcal{N}_{X_{t-\tau}}^{Y_t}))$ the conditions in MITP, it can be expressed as

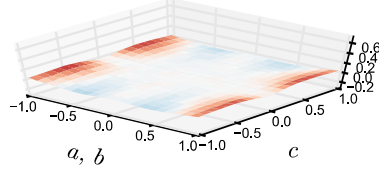
a) ITX



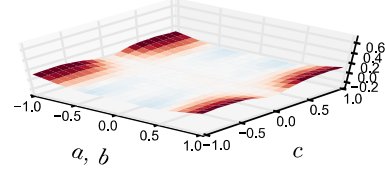
MITP



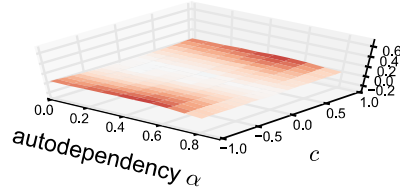
IIX



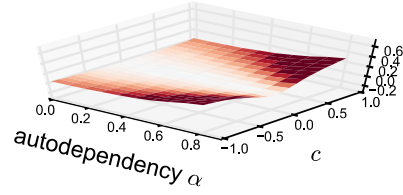
MII



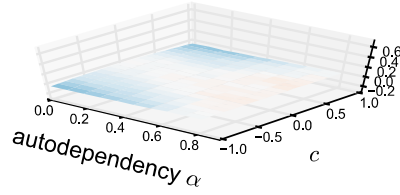
b) ITX



MITP



IIX



MII

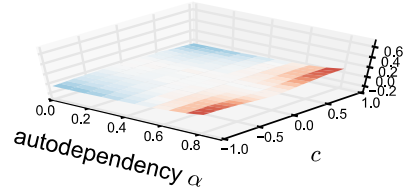


Figure 6. Same as in Fig. 5, but for the nonlinear model (34).

$$\forall W_{t-\tau_i}^{(i)} \in \mathcal{C}_{X_{t-\tau} \rightarrow Y_t} : \\ I(W_{t-\tau_i}^{(i)}; \mathcal{S}^{\text{MITP}} \setminus \mathcal{P}_{W_{t-\tau_i}^{(i)}} | \mathcal{P}_{W_{t-\tau_i}^{(i)}}) = 0, \quad (40)$$

which essentially isolates the ‘dynamical noise’ and tests for its contemporaneous independence with any of the conditions on external processes involved in MITP. Note that $X_{t-\tau}$ is also included in $\mathcal{C}_{X_{t-\tau} \rightarrow Y_t}$ and that we denote by $W_{t-\tau_i}^{(i)}$ each individual subprocess along causal paths at a certain lag τ_i . If one subprocess occurs at multiple lags, it will still have another index i .

Theorem 2 (Coupling strength autonomy for MITP). *Let X, Y be two subprocesses of a multivariate stationary discrete-time process \mathbf{X} sufficing the Markov property (Eq. (15)) with time series graph \mathcal{G} . We assume that $X_{t-\tau}, Y_t$ are connected by a directed path with path nodes $\mathcal{C}_{X_{t-\tau} \rightarrow Y_t}$ including $X_{t-\tau}$ as defined in Eq. (21). We denote those parents of Y_t that are in the path nodes as $\mathcal{P}_Y^{\mathcal{C}} = \mathcal{P}_{Y_t} \cap \mathcal{C}_{X_{t-\tau} \rightarrow Y_t}$*

and correspondingly for other path nodes and assume the following dependencies:

$$X_t = g_X(\mathcal{P}_{X_{t-\tau}}) + \eta_t^X \\ Y_t = f_Y(\mathcal{P}_Y^{\mathcal{C}}) + g_Y(\mathcal{P}_{Y_t} \setminus \mathcal{P}_Y^{\mathcal{C}}) + \eta_t^Y, \quad (41)$$

where f_Y is linear and g_Y arbitrary. Further, for all path nodes $W^{(i)}$ we assume the dependencies

$$W_t^{(i)} = f_i(\mathcal{P}_i^{\mathcal{C}}) + g_i(\mathcal{P}_i \setminus \mathcal{P}_i^{\mathcal{C}}) + \eta_t^i \\ \forall W^{(i)} \in \mathcal{C}_{X_{t-\tau} \rightarrow Y_t} \setminus \{X_{t-\tau}\}, \quad (42)$$

where the f_i are again linear, the g_i are arbitrary functions and the dynamical noise terms η^i are i.i.d. due to Markovity. Then, MITP (Eq. (24)) is given by

VI. DISCUSSION

A. Relation to linear causal effect theory

We phrased the idea of causal influence in an information-theoretic setting. Pearl's theory of causal effects [19, 21] can also be embedded in the time series graph framework [63]. Assuming the time series graph is causally sufficient [19] and all dependencies are linear, causal effects can simply be derived from multivariate regressions. Firstly, in analogy to ITY or MIT as a measure of direct link strength, the *path coefficient* of a link is given by the corresponding (typically standardized) coefficient in a multivariate regression of each process on its parents in the time series graph [79]. Further, in analogy to ITX or MITP, the linear causal effect of $X_{t-\tau}$ on Y_t also via indirect paths can be estimated by a standardized regression of Y on the multiple regressors $\{X_{t-\tau}, \mathcal{P}(X_{t-\tau})\}$. The linear *Causal Effect* (CE) [19, 21] is then given by the corresponding (standardized) regression coefficient r belonging to $X_{t-\tau}$,

$$\text{CE}_{X \rightarrow Y}(\tau) = r_{Y_t | X_{t-\tau}, \mathcal{P}(X_{t-\tau})}. \quad (48)$$

This formulation assumes the “no contemporaneous dependency”-condition (40) for simplicity, but it can be generalized. The causal effect $\text{CE}_{X \rightarrow Y}(\tau)$ quantifies the change in the expectation of Y_t (in units of its standard deviation) induced by raising the lagged $X_{t-\tau}$ by one standard deviation, while keeping the parents of $X_{t-\tau}$ constant. Then the total causal effect between lagged processes is simply given by the sum over the product of path coefficients along each causal paths connecting $X_{t-\tau}$ and Y_t . For example, for the model (29) with time series graph in Fig. 5(a) the total linear causal effect between X_{t-2} and Y_t is given by $\sqrt{\frac{\Gamma_X}{\Gamma_Y}}(c+ab)$, where $\sqrt{\Gamma}$ is the normalization by the standard deviations which, however, depends on the autodependency strength and other coefficients here. ITX is simply the mutual information with the same conditions as CE (for no neighbors), while MITP for this model example (see Eq. (44) or Eq. (32)) is $\frac{1}{2} \ln \left(1 + \frac{(c+ab)^2 \sigma_X^2}{b^2 \sigma_W^2 + \sigma_Y^2} \right)$. ITX, MITP and CE all depend on the ‘coupling mechanism’ ($c+ab$), but with different ‘normalizations’.

Even in linear models, the *Mediated Causal Effect* (MCE) is more difficult to identify [19, 80]. The causal interpretation is that an indirect effect via the node(s) W measures the increase we would see in Y_t while holding $X_{t-\tau}$ and all other intermediate nodes and parents of $X_{t-\tau}$ constant and increasing the node(s) W to whatever value it would obtain under a unit change in $X_{t-\tau}$ while holding the parents of $X_{t-\tau}$ constant [19, 80]. To identify MCE for the triplet case in model (29) with time series graph in Fig. 5(a) one can subtract from CE the contribution of all paths *not* passing through W :

$$\begin{aligned} I_{X \rightarrow Y}^{\text{MITP}}(\tau) = & I(\eta_{t-\tau}^X; \eta_t^Y + f(\eta_{t-\tau}^X, \cup_i \eta_{t-\tau_i}^i)) \\ & | \mathcal{P}_{Y_t} \setminus \mathcal{C}_{X_{t-\tau} \rightarrow Y_t}, \mathcal{P}(\mathcal{C}_{X_{t-\tau} \rightarrow Y_t}), \mathcal{N}_{X_{t-\tau}}^{Y_t}, \mathcal{P}(\mathcal{N}_{X_{t-\tau}}^{Y_t}) \end{aligned} \quad (43)$$

where $0 < \tau_i < \tau \forall i$. If further the “no contemporaneous dependency”-condition (40) holds, MITP reduces to a mutual information

$$I_{X \rightarrow Y}^{\text{MITP}}(\tau) = I(\eta_{t-\tau}^X; \eta_t^Y + f(\eta_{t-\tau}^X, \cup_i \eta_{t-\tau_i}^i)), \quad (44)$$

where f is a linear function and $\cup_i \eta^i$ denotes the innovation terms or dynamical noise of all path nodes in $\mathcal{C}_{X_{t-\tau} \rightarrow Y_t} \setminus \{X_{t-\tau}\}$.

The proof is given in Appendix B 3. This theorem also includes the coupling strength autonomy theorem for MIT [39] as a special case if $\mathcal{C}_{X_{t-\tau} \rightarrow Y_t} = \{X_{t-\tau}\}$ and under the “no sidepath”-constraint in Ref. [39], then $f(\eta_{t-\tau}^X, \cup_i \eta_{t-\tau_i}^i) = f(\eta_{t-\tau}^X)$.

Since momentary interaction information (MII) is the difference between MITP and the MITP conditioned on one of the path nodes (excluding $X_{t-\tau}$), the theorem follows from the above theorem.

Theorem 3 (Coupling strength autonomy for MII). *Using the same assumptions as for Theorem 2, the momentary interaction information $\mathcal{I}_{X \rightarrow Y | \mathbf{W}}^{\text{MII}}(\tau)$ between $X_{t-\tau}$, Y_t and one or more intermediate processes $\mathbf{W} = (W_{t-\tau_1}^{(1)}, W_{t-\tau_2}^{(2)} \dots) \in \mathcal{C}_{X_{t-\tau} \rightarrow Y_t} \setminus \{X_{t-\tau}\}$ indexed by j reduces to*

$$\begin{aligned} \mathcal{I}(\eta_{t-\tau}^X; \eta_t^Y + f(\eta_{t-\tau}^X, \cup_i \eta_{t-\tau_i}^i); \\ \left\{ \eta_{t-\tau_j}^j + f_j(\eta_{t-\tau}^X, \cup_{i \neq j} \eta_{t-\tau_i}^i) \right\}_j \\ | \mathcal{P}_{Y_t} \setminus \mathcal{C}_{X_{t-\tau} \rightarrow Y_t}, \mathcal{P}(\mathcal{C}_{X_{t-\tau} \rightarrow Y_t}), \mathcal{N}_{X_{t-\tau}}^{Y_t}, \mathcal{P}(\mathcal{N}_{X_{t-\tau}}^{Y_t}) \end{aligned} \quad (45)$$

and, if further the “no contemporaneous dependency”-condition (40) holds, to

$$\begin{aligned} \mathcal{I}(\eta_{t-\tau}^X; \eta_t^Y + f(\eta_{t-\tau}^X, \cup_i \eta_{t-\tau_i}^i); \\ \left\{ \eta_{t-\tau_j}^j + f_j(\eta_{t-\tau}^X, \cup_{i \neq j} \eta_{t-\tau_i}^i) \right\}_j \end{aligned} \quad (46)$$

for linear functions f, f_j .

The proof is given in Appendix B 4. For the case of a causal triple as shown in Fig. 5 this further reduces to

$$\mathcal{I}(\eta_{t-\tau}^X; \eta_t^Y + (c+ab)\eta_{t-\tau}^X + b\eta_{t-\tau_W}^W; \eta_{t-\tau_W}^W + a\eta_{t-\tau}^X), \quad (47)$$

from which the special case with Gaussian innovations Eq. (33) follows.

$$\begin{aligned}
& \text{MCE}_{X \rightarrow Y|W}(\tau = 2) \\
&= \text{CE}_{X \rightarrow Y}(2) - \underbrace{r_{Y_t X_{t-2} \cdot \mathcal{P}(X_{t-2}), W_{t-1}, \mathcal{P}(W_{t-1})}}_{\text{CE excluding paths through } W} \\
&= \sqrt{\frac{\Gamma_X}{\Gamma_Y}} ab. \tag{49}
\end{aligned}$$

Note the additional condition on the parents of W here needed to exclude a confounding of the mediating link from W to Y from the past due to W_{t-2} . This is also the idea behind the interaction information MII which is conditioned on the parents of all intermediate processes to exclude possible confounding. MII is given also by a difference, but of CMIs instead of regressions: $\frac{1}{2} \ln \left(1 + \frac{(c+ab)^2 \sigma_X^2}{b^2 \sigma_W^2 + \sigma_Y^2} \right) - \frac{1}{2} \ln \left(1 + \frac{c^2 \sigma_X^2 \sigma_W^2}{(\sigma_W^2 + a^2 \sigma_X^2) \sigma_Y^2} \right)$, where the latter term information-theoretically quantifies the strength of the direct link with coefficient c . The linear framework allows for quantifying the relative influence of paths between two processes by the ‘locally’ estimated weights making it easy to interpret, but it rests on a linear assumption. Another advantage of the linear approach is that total and indirect effects can also be investigated in the frequency domain in the framework of *directed transfer functions* [22–24]. To some extent causal effects can also be estimated for more general nonlinear structural equation models [19, 81], but especially mediated effects are difficult to identify if no strong assumptions are fulfilled [80].

B. Coupling strength autonomy

MIT, MITP and MII somewhat disentangle the coupling structure, which is exactly the coupling strength autonomy that makes these measures well-interpretable as measures that solely depend on the “coupling mechanism” between $X_{t-\tau}$ and Y_t (and possibly intermediate processes) as shown in the previous sections, autonomous of other external processes. One such possible misleading input “filtered out” is autocorrelation, or, more generally, autodependency as has been shown in the model examples. This interpretability is facilitated by the careful conditioning on all possible confounding processes which can be determined from the time series graph (assuming the graph entails all relevant processes, i.e., causal sufficiency [19]). In a way, coupling strength autonomy is an information-theoretic description similar to the identifiability of causal effects in Pearl’s framework, but this connection needs to be further investigated.

However, the assumptions allowing for such an interpretability are quite restrictive: While arbitrary additive functional dependencies of the interaction processes on external drivers can be conditioned out, the whole interaction mechanism from X to Y via intermediate processes needs to be linear. Note that this does not imply that linear measures can be used instead, because these would not exclude arbitrary nonlinear external drivers. A further complication is that the potentially high dimensionality due to many external drivers leads to a strong bias in MITP and MII, even

for the most advanced information-theoretic estimators employed here [51, 52]. These limitations hamper the added value in interpretability of MITP and MII compared to ITX / IIX. But if no detailed knowledge of the dynamical equations are given, this approach at least is rigorously based on the time series graph encoding the Markovian conditional independence structure as an abstraction of the dynamics. Also if the equations are known, but feature highly complex chaotic behavior like toy models from nonlinear dynamics, plots of the measures introduced here like in Figs. 5, 6 can help to better understand information transfer in dynamical interactions.

C. Information transfer and complex network theory

In the literature of neuroscience [1, 82, 83] and recently also in climate research [3, 84], multivariate datasets are often analyzed using pairwise association measures combined with complex network theory [85]. Networks are typically reconstructed by thresholding the association matrix (either by some predefined threshold or such that a fixed link density is obtained). In interpreting such networks, it is important to take into account the aspect that the network comes from only pairwise associations. For example, the basic principle of transitivity of correlation leads to a lot of spurious links strongly affecting network measures such as the average path length. Typically, short-path lengths in these networks are related to the global efficiency of information transfer, e.g., in the brain [1], but also in climate [2]. But the authors in Refs. [86, 87] have shown that even for a set of entirely independent processes a small world topology (i.e., small average path length and high clustering of the network) emerges. Further, the robustness of a system to random error or perturbations is typically associated with a high clustering coefficient. Also this measure can lead to false interpretations if causality is not taken into account: For example, for the true causal relations $X \rightarrow Y \rightarrow Z$, there are significant correlations between all pairs and the clustering coefficient of the non-causal network would be maximal. In this simple example an ‘attack’ on node Y in the center certainly disrupts the causal network most because it also destroys the interlink between X and Z . But this is not taken into account if the non-causal network is analyzed. In recent years some studies in neuroscience have also applied linear Granger causality methods [88, 89] and bivariate transfer entropy has been applied to climate time series [5].

With the measures ITX / MITP and IIX / MII, one can make an attempt to put the notion of shortest paths in an information-theoretic perspective. Instead of counting shortest paths between X and Y , ITX or MITP give an appropriate measure of how much information is actually transferred. The interaction informations IIX or MII can then be seen as an alternative to *betweenness centrality* [85, 90] defined as

$$\mathcal{B}(k) = \sum_{i \neq k \neq j} \frac{n_{sp}(k)}{n_{sp}}, \tag{50}$$

where n_{sp} is the total number of shortest paths from node i to node j and $n_{sp}(k)$ is the number of those paths that pass through k . In analogy, one can define an aggregated IIX node measure, *causal interaction betweenness* (CIB), as

$$\mathcal{I}^{\text{CIB}}(k) = \frac{1}{|\mathcal{C}_k|} \sum_{(i,j,\tau) \in \mathcal{C}_k} |\mathcal{I}_{i \rightarrow j|k}^{\text{IIX}}(\tau)|, \quad (51)$$

where \mathcal{C}_k is the set of interactions between all non-identical pairs of processes (i, j) at all lags $0 < \tau \leq \tau_{\max}$ where $k \neq i, j$ is an intermediate process (at any lags) and $|\mathcal{C}_k|$ denotes the number of all interactions. Here we take the absolute value $|\mathcal{I}_{i \rightarrow j|k}^{\text{IIX}}(\tau)|$, but one could further distinguish between enhancing (positive interaction information) and counteracting (negative interaction information) effects. A linear application of such an approach is discussed in Ref. [10]. Instead of IIX, also MII can be used to exclude further biasing confounders at the price of a much higher estimation dimension. Note that $|\mathcal{I}_{i \rightarrow j|k}^{\text{IIX}}(\tau)|$ does *not* denote a fraction like $\frac{n_{sp}(k)}{n_{sp}}$ and a more analogous measure to betweenness centrality would be obtained by normalizing each summand in Eq. (51) by the corresponding ITX or MITP,

$$\bar{\mathcal{I}}^{\text{CIB}}(k) = \frac{1}{|\mathcal{C}_k|} \sum_{(i,j,\tau) \in \mathcal{C}_k} \frac{|\mathcal{I}_{i \rightarrow j|k}^{\text{IIX}}(\tau)|}{I_{i \rightarrow j}^{\text{ITX}}(\tau)}, \quad (52)$$

which is, however, not robust to outliers for small ITX.

VII. APPLICATION TO CLIMATOLOGICAL TIME SERIES

To illustrate the causal pathway analysis also on real data, we analyze a climatological dataset of daily mean sea level pressure anomalies (time series with the seasonal cycle removed) in the winter months (November to April) of 1997–2003 [91] at four locations in Eastern Europe indicated as A, B, C, D on the map in Fig. 7(d) which was also analyzed in [20]. Figure 7(a) depicts the time series.

The reconstruction of the causal links with the PC-algorithm was discussed in Ref. [20], here we use it in a two-step approach as recommended in Sect. III. First, we estimate the preliminary parents and neighbors of all four variables as in Ref. [20] using a fixed significance threshold $I^* = 0.015 \text{ nats}$. These are $\tilde{\mathcal{P}}_A = \{A_{t-1}, B_{t-1}\}$, $\tilde{\mathcal{N}}_A = \{C_t\}$, $\tilde{\mathcal{P}}_B = \{B_{t-1}, D_{t-1}\}$, $\tilde{\mathcal{N}}_B = \{D_t\}$, $\tilde{\mathcal{P}}_C = \{C_{t-1}, D_{t-1}\}$, $\tilde{\mathcal{N}}_C = \{A_t\}$, $\tilde{\mathcal{P}}_D = \{D_{t-1}\}$, and $\tilde{\mathcal{N}}_D = \{B_t\}$. Secondly, we use these parents and neighbors to estimate MIT values for all links which are plotted in Fig. 7(b) next to MI. Also contemporaneous MIT values using also neighbors as a condition as defined in Ref. [39] are shown. MIT values above the same fixed significance threshold $I^* = 0.015 \text{ nats}$ are now considered as the causal links (directed and contemporaneous for $\tau = 0$) defining the time series graph shown in Fig. 7(c). Note that contemporaneous links do not disappear if

the contemporaneous neighbors are excluded from the condition in MIT (corresponding to dashed links in Def. 12). From this graph one can now read off the parents \mathcal{P} and neighbors \mathcal{N} used in the path-based information transfer measures. This graph also helps to understand why MI has strongly significant values in Fig. 7(b) where MIT is zero. For example, the MI values in panel $C \rightarrow D$ can well be explained by past values of D , e.g., D_{t-2} acting as a common driver via $D_t \leftarrow D_{t-1} \leftarrow D_{t-2} \rightarrow C_{t-1}$.

In the following, we conduct a causal path analysis for the influence of D on A and C at different lags. There are significant ITX values at two and three days lag (Fig. 7(b)). From the time series graph (Fig. 7(c)) we can read off the causal paths contributing to the ITX values. In Tab. I we list the results of an analysis for three causal path interactions. The interaction $D_{t-2} \rightarrow \dots \rightarrow A_t$ has only one causal path via B_{t-1} , but also contemporaneous sidepaths $D_{t-2} - B_{t-2} \rightarrow \dots \rightarrow A_t$. Here ITX and IIX gave very noisy results. MITP, on the other hand, is larger than ITX (as expected from Theorem 1) with a much smaller confidence interval. Here MII via B_{t-1} explains all of the MITP within error bounds as expected since it is the only intermediate node and no direct link exists. Next, we turn to the more interesting influence of D on C . At a lag of two days MITP is slightly smaller than ITX, which, as discussed in Sect. V A, can be due to finite sample bias. The indirectness of the interaction $D_{t-2} \rightarrow \dots \rightarrow C_t$ here stems from the two paths $D_{t-2} \rightarrow D_{t-1} \rightarrow C_t$ and $D_{t-2} \rightarrow C_{t-1} \rightarrow C_t$ via autodependencies (Fig. 7(c)). The interaction analyses with IIX and MII here both indicate that a slightly larger part of the ITX is mediated via D_{t-1} rather than C_{t-1} (Tab. I) in line with the higher auto-MIT strength of the autodependency within D . At a lag of three days the interaction $D_{t-3} \rightarrow \dots \rightarrow C_t$ has many more paths not only via autodependencies, but also via B_{t-2} and A_{t-1} (and also non-causal contemporaneous sidepaths). While also here the auto-dependencies together with the direct link $D_{t-1} \rightarrow C_t$ strongly contribute to ITX (Tab. I), the path $D_{t-3} \rightarrow B_{t-2} \rightarrow A_{t-1} \rightarrow C_t$ seems to be relevant, too, as indicated by the significant IIX and MII values through these nodes.

This causal picture of a counter-clockwise ‘flow of entropy’ is consistent with the dynamical processes governing the lower and middle atmosphere circulation in the considered area. One usually observes a superposition of westerly winds with traveling extratropical counter-clockwise cyclones that traverse the area and whose trajectories are regulated by the aforementioned westerlies [92]. Consistent with the causal lags of one or two days, these processes act on short daily time scales. Note that the variables were defined in an ad-hoc manner by the locations of grid points here, but one can better isolate subprocesses of complex systems by a suitable dimension reduction, see [10, 93] for an application to the atmospheric pressure system.

VIII. CONCLUSIONS

This work expanded the approach introduced in Ref. [39] which considered information-theoretic measures to quantify

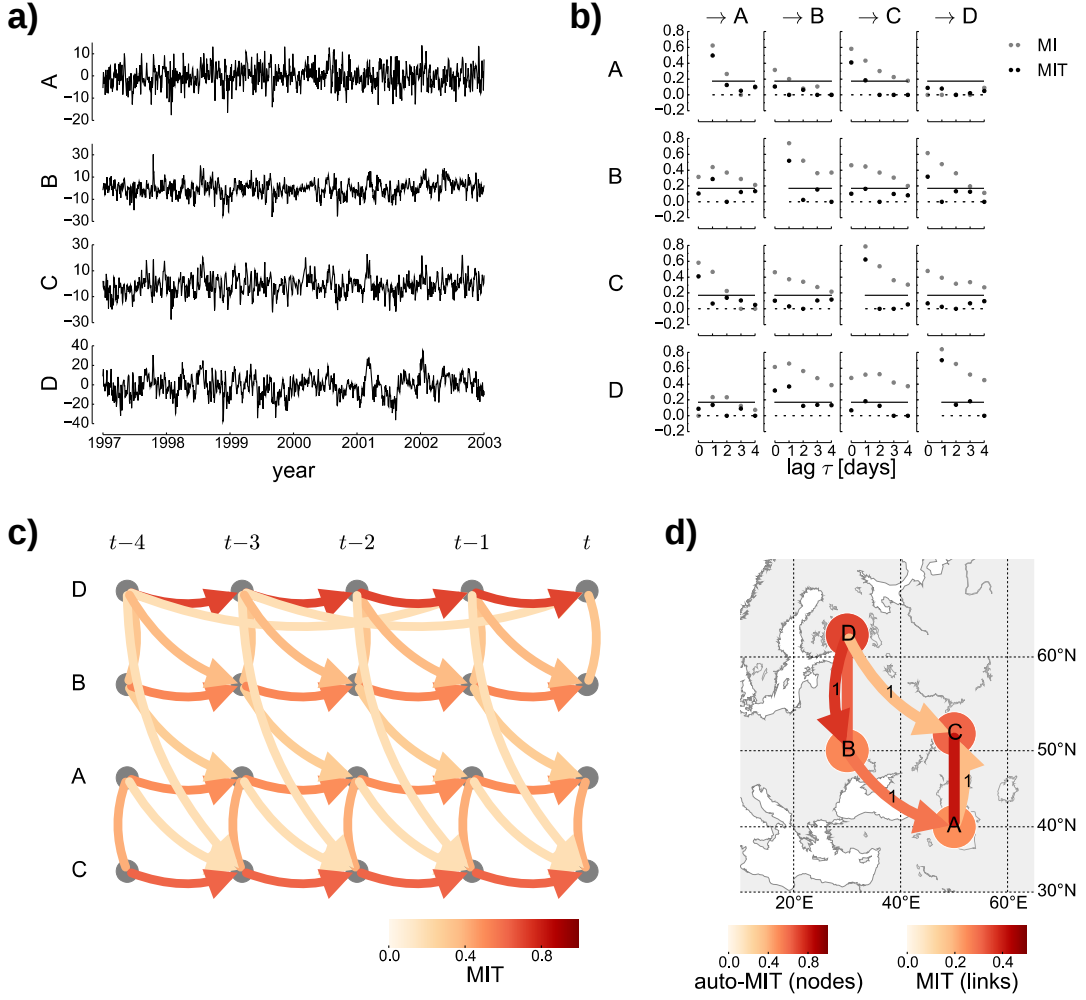


Figure 7. Analysis of daily time series of mean sea level pressure with $T = 1268$ days. The algorithm to estimate the parents and neighbors was run as in Ref. [20] using a threshold $I^* = 0.015$ *nats*, $\tau_{\max} = 4$ days and the CMI nearest-neighbor parameter $k = 100$ (larger k have smaller variance which is important for independence tests). (a) Anomaly time series (days in winter months November to April only) of the four variables, all units are in hectopascal (hPa) relative to the seasonal mean. (b) Lag functions of MI and multivariate MIT, here a parameter $k = 10$ was chosen to reduce the bias. Also contemporaneous MITs as defined in Ref. [39] are shown. All (C)MI values have been rescaled to the (partial) correlation scale via $I \rightarrow \sqrt{1 - e^{-2I}} \in [0, 1]$ [4]. The solid lines denote the fixed threshold $I^* = 0.015$ (rescaled), which is used to define the time series graph for the path-analysis. (c) shows the time series graph with the edge color denoting the rescaled MIT strength. Note the different order of the variables to better visualize the causal paths. Repetitions of links emanating from times further than $t - 4$ in the past are omitted. (d) aggregated visualization as process graph (labels denote the lags and edge and node colors correspond to cross-MIT and auto-MIT, respectively, at the lag with maximum value).

the strength of links in causal time series graphs. Here the goal was to quantify indirect causal interactions and how much intermediate processes mediate or counteract an interaction. The two considered classes of measures ITX / IIX and MITP / MII for a causal interaction $X_{t-\tau} \rightarrow \dots \rightarrow Y_t$ have in common the idea to extract information originating in process X only at the lagged time $t - \tau$ and are conditioned in order to measure only information transfer along causal paths. MITP further attempts to exclude the influence of other drivers of Y or intermediate path nodes by conditioning out the parents of all processes involved in the causal interaction. As a fur-

ther step, IIX and MII quantify the mediating or counteracting effect of intermediate processes on causal paths to an interaction mechanism to determine the relative importance of pathways of causal information transfer. In extensions of the coupling strength autonomy theorem [39], for certain model classes MITP and MII allow to entirely isolate the quantification of the interaction mechanism from other driving mechanisms. Then the values of MITP and MII can be solely related to the coefficients belonging to the indirect interaction mechanism between X and Y making them well interpretable not only information-theoretically, but also relating their value to

Causal path	ITX	IIX	MITP	MII
$D_{t-2} \rightarrow \dots \rightarrow A_t$ via B_{t-1}	0.09 ± 0.06	0.00 ± 0.06	0.15 ± 0.02	0.14 ± 0.02
$D_{t-2} \rightarrow \dots \rightarrow C_t$ via D_{t-1} via C_{t-1}	0.26 ± 0.02	0.22 ± 0.02 0.16 ± 0.02	0.24 ± 0.02	0.23 ± 0.02 0.18 ± 0.02
$D_{t-3} \rightarrow \dots \rightarrow C_t$ via (D_{t-2}, D_{t-1}) via B_{t-2} via A_{t-1} via (C_{t-2}, C_{t-1})	0.25 ± 0.02	0.22 ± 0.02 0.15 ± 0.02 0.09 ± 0.02 0.22 ± 0.02	0.22 ± 0.02	0.21 ± 0.02 0.13 ± 0.02 0.12 ± 0.02 0.20 ± 0.02

Table I. Measures of information transfer along selected causal paths for the climatological example of Fig. 7. All (C)MI values have been rescaled to the (partial) correlation scale via $I \rightarrow \sqrt{1 - e^{-2I}} \in [0, 1]$ [4]. The estimation parameter $k = 10$ was chosen as a compromise between low bias and not too high variance, the 68% confidence interval is based on a bootstrap [76] with 1000 samples.

the underlying dynamics.

Generally, however, the value of MIT or MITP remains hard to interpret for nonlinearly intertwined complex systems, but their information-theoretic definition and foundation based on the Markov structure of the process allows to quantify a rigorous notion of causal information transfer as an abstraction of the dynamics. The novel measures can also be helpful in understanding dynamical interactions in toy models from nonlinear dynamics. While the absolute values of ITX and MITP, measured in *nats*, cannot be simply related to units of the variables, the values of the interaction measures IIX and MII can be used to quantify how much of the information transfer can be attributed to individual intermediate processes. The goal of information-theoretic measures is not a complete understanding of the dynamics of the system which can only be achieved by experiments or detailed modeling. Then causal effect quantifiers such as proposed in Pearl [19] or [53] are good starting points.

The climatological analysis underlines the importance of inferring mechanism delays and pathways for physical interpretations and serves as a first step to study more complex systems in climate and beyond. More exploratory studies in the spirit of functional network analysis, but with a rigorous

definition of information transfer, can be based on the aggregate measures introduced in Sect. VIC. A linear application of such an approach is demonstrated in Ref. [10]. As a further outlook, it will be an interesting avenue of research to connect the time series graph-based framework of information transfer to recent concepts of *synergistic information sharing* [77, 78]. In Ref. [73] synergistic effects are studied with respect to optimal prediction schemes.

ACKNOWLEDGMENTS

The early stages of this work benefited from discussions with Bernd Pompe and Jobst Heitzig. Vladimir Petoukhov helped in interpreting the climatological example. This work was supported by the German National Academic Foundation, a Humboldt University Postdoctoral Fellowship and the German Federal Ministry of Science and Education (Young Investigators Group CoSy-CC², grant no. 01LN1306A). A *Python* script to estimate the causal network can be obtained from the author's website at www.pik-potsdam.de/members/jakrunge.

The author declares no conflict of interest.

-
- [1] E. Bullmore and O. Sporns, *Nature reviews. Neuroscience* **10**, 186 (2009).
 - [2] A. A. Tsonis, K. L. Swanson, and G. Wang, *Journal of Climate* **21**, 2990 (2008).
 - [3] J. F. Donges, Y. Zou, N. Marwan, and J. Kurths, *European Physical Journal: Special Topics* **174**, 157 (2009).
 - [4] T. M. Cover and J. A. Thomas, *Elements of Information Theory* (John Wiley & Sons, Hoboken, 2006).
 - [5] J. Hlinka, D. Hartman, M. Vejmelka, J. Runge, N. Marwan, J. Kurths, and M. Paluš, *Entropy* **15**, 2023 (2013).
 - [6] Y. Deng and I. Ebert-Uphoff, *Geophysical Research Letters* **41**, 193 (2014).
 - [7] C. F. Schleussner, J. Runge, J. Lehmann, and A. Levermann, *Earth System Dynamics* **5**, 103 (2014).
 - [8] G. Balasis, R. Donner, S. Potirakis, J. Runge, C. Papadimitriou, I. Daglis, K. Eftaxis, and J. Kurths, *Entropy* **15**, 4844 (2013).
 - [9] T. Zerenner, P. Friederichs, K. Lehnertz, and A. Hense, *Chaos: An Interdisciplinary Journal of Nonlinear Science* **24**, 023103 (2014).
 - [10] J. Runge, V. Petoukhov, J. F. Donges, J. Hlinka, N. Jajcay, M. Vejmelka, D. Hartman, N. Marwan, M. Paluš, and J. Kurths, under review at *Nature Communications* (2015).
 - [11] G. Niso, R. Bruña, E. Pereda, R. Gutiérrez, R. Bajo, F. Maestú, and F. Del-Pozo, *Neuroinformatics* **11**, 405 (2013).
 - [12] M. Wibral, R. Vicente, and M. Lindner, in *Springer*, edited by M. Wibral, R. Vicente, and J. Lizier (Springer Berlin Heidelberg, Berlin, 2014), chap. 1.
 - [13] K. Lehnertz and H. Dickten, *Philosophical Transactions of the Royal Society of London A* **373** (2015).
 - [14] L. Faes, G. Nollo, and A. Porta, *Physical Review E* **83**, 051112 (2011).
 - [15] L. Faes, D. Marinazzo, A. Montalto, and G. Nollo, *IEEE Transactions on Biomedical Engineering* **61**, 2556 (2014).
 - [16] J. Runge, M. Riedl, H. Stepan, N. Wessel, and J. Kurths, *Phys-*

- iological Measurement **36**, 813 (2015).
- [17] C. W. J. Granger, *Econometrica* **37**, 424 (1969).
 - [18] P. Spirtes, C. Glymour, and R. Scheines, *Causation, Prediction, and Search*, vol. 81 (The MIT Press, Boston, 2000).
 - [19] J. Pearl, *Causality: models, reasoning, and inference* (Cambridge University Press, Cambridge, 2000).
 - [20] J. Runge, J. Heitzig, V. Petoukhov, and J. Kurths, *Physical Review Letters* **108**, 258701 (2012).
 - [21] J. Pearl, *Journal of Causal Inference* **1**, 155 (2013).
 - [22] M. Kaminski, M. Ding, W. A. Truccolo, and S. L. Bressler, *Biological Cybernetics* **85**, 145 (2001).
 - [23] A. Korzeniewska, M. Manczak, M. Kaminski, K. J. Blinowska, and S. Kasicki, *Journal of Neuroscience Methods* **125**, 195 (2003).
 - [24] K. J. Blinowska and M. Kaminski, in *Handbook of Time Series Analysis*, edited by J. T. Björn Schelter, Matthias Winterhalder (John Wiley & Sons, 2006), chap. 15.
 - [25] L. A. Baccalá and K. Sameshima, *Biological cybernetics* **84**, 463 (2001).
 - [26] B. Schelter, M. Winterhalder, M. Eichler, M. Peifer, B. Hellwig, B. Guschlbauer, C. H. Lücking, R. Dahlhaus, and J. Timmer, *Journal of Neuroscience Methods* **152**, 210 (2006).
 - [27] M. Jachan, K. Henschel, J. Nawrath, A. Schad, J. Timmer, and B. Schelter, *Physical Review E* **80**, 011138 (2009).
 - [28] L. Sommerlade, M. Eichler, M. Jachan, K. Henschel, J. Timmer, and B. Schelter, *Physical Review E* **80**, 051128 (2009).
 - [29] B. Schelter, J. Timmer, and M. Eichler, *Journal of neuroscience methods* **179**, 121 (2009).
 - [30] Y. Chen, G. Rangarajan, J. Feng, and M. Ding, *Physics Letters A* **324**, 26 (2004).
 - [31] D. Marinazzo, M. Pellicoro, and S. Stramaglia, *Physical Review Letters* **100**, 144103 (2008).
 - [32] T. Schreiber, *Physical Review Letters* **85**, 461 (2000).
 - [33] J. T. Lizier and M. Prokopenko, *The European Physical Journal B* **73**, 605 (2010).
 - [34] M. Wibral, N. Pampu, V. Priesemann, F. Siebenhühner, H. Seiwert, M. Lindner, J. T. Lizier, and R. Vicente, *PloS one* **8**, e55809 (2013).
 - [35] F. Abdul Razak and H. J. Jensen, *PLoS ONE* **9** (2014).
 - [36] L. Faes, D. Kugiumtzis, G. Nollo, F. Jurysta, and D. Marinazzo, *Physical Review E* **91**, 032904 (2015).
 - [37] H. Dickten and K. Lehnertz, *Physical Review E* **90**, 062706 (2014).
 - [38] B. Pompe and J. Runge, *Physical Review E* **83**, 051122 (2011).
 - [39] J. Runge, J. Heitzig, N. Marwan, and J. Kurths, *Physical Review E* **86**, 061121 (2012).
 - [40] J. Runge, *ArXiv e-prints* p. e55809 (2013).
 - [41] D. Kugiumtzis, *Physical Review E* **87**, 062918 (2013).
 - [42] J. Sun, C. Cafaro, and E. Boltt, *Entropy* **16**, 3416 (2014).
 - [43] J. Sun, D. Taylor, and E. M. Boltt, *SIAM Journal on Applied Dynamical Systems* **14**, 27 (2014).
 - [44] C. Cafaro, W. Lord, J. Sun, and E. Boltt, *Chaos: An Interdisciplinary Journal of Nonlinear Science* **25**, 043106 (2015).
 - [45] S. L. Lauritzen, *Graphical models* (Oxford University Press, Oxford, 1996).
 - [46] M. Eichler, *Probability Theory and Related Fields* **153**, 233 (2012).
 - [47] D. Chicharro and S. Panzeri, *Frontiers in Neuroinformatics* **8**, 1 (2014).
 - [48] P. Spirtes and C. Glymour, *Social Science Computer Review* **9**, 62 (1991).
 - [49] I. Ebert-Uphoff and Y. Deng, *Journal of Climate* **25**, 5648 (2012).
 - [50] J. Runge, V. Petoukhov, and J. Kurths, *Journal of Climate* **27**, 720 (2014).
 - [51] A. Kraskov, H. Stögbauer, and P. Grassberger, *Physical Review E* **69**, 066138 (2004).
 - [52] S. Frenzel and B. Pompe, *Physical Review Letters* **99**, 204101 (2007).
 - [53] D. A. Smirnov, *Physical Review E* **90**, 062921 (2014).
 - [54] IPCC, *Climate Change 2013: The Physical Science Basis. Contribution of Working Group I to the Fifth Assessment Report of the Intergovernmental Panel on Climate Change* (Cambridge University Press, Cambridge, 2013).
 - [55] X. S. Liang, *Physical Review E* **90**, 052150 (2014).
 - [56] X. S. Liang, *ArXiv e-prints* p. 1501.03548v2 (2015).
 - [57] N. Ay and D. Polani, *Advances in complex systems* **11**, 17 (2008).
 - [58] D. Janzing, D. Balduzzi, M. Grosse-Wentrup, and B. Schölkopf, *The Annals of Statistics* **41**, 2324 (2013).
 - [59] C. E. Shannon, *Bell System Technical Journal* **27**, 379 (1948).
 - [60] C. E. Shannon and W. Weaver, *The Mathematical Theory of Communication* (University of Illinois Press, Urbana, 1963).
 - [61] T. Schreiber and H. Kantz, *Chaos: An Interdisciplinary Journal of Nonlinear Science* **5**, 133 (1995).
 - [62] J. P. Florens and M. Mouchart, *Econometrica: Journal of the Econometric Society* **50**, 583 (1982).
 - [63] M. Eichler and V. Didelez, *Lifetime data analysis* **16**, 3 (2010).
 - [64] S. Kullback and R. A. Leibler, *The Annals of Mathematical Statistics* **22**, 79 (1951).
 - [65] N. Abramson, *Information theory and coding* (McGraw-Hill, New York, NY, 1963).
 - [66] T. Tsujishita, *Advances in Applied Mathematics* **16**, 269 (1995).
 - [67] L. Leydesdorff and Y. Sun, *Journal of the American Society for Information Science and Technology* **60**, 778 (2009).
 - [68] W. J. McGill, *Psychometrika* **19**, 97 (1954).
 - [69] A. Jakulin and I. Bratko, *Analyzing attribute dependencies* (Springer, New York, 2003).
 - [70] S. Frenzel and B. Pompe, *Physical Review Letters* **99**, 204101 (2007).
 - [71] R. Dahlhaus, *Metrika* **51**, 157 (2000).
 - [72] J. Runge, J. Heitzig, V. Petoukhov, and J. Kurths, *Physical Review Letters* **108**, 258701 (2012).
 - [73] J. Runge, R. V. Donner, and J. Kurths, *Physical Review E* **91**, 052909 (2015).
 - [74] C. Uhler, G. Raskutti, P. Bühlmann, and B. Yu, *The Annals of Statistics* **41**, 436 (2013).
 - [75] L. Barnett, A. B. Barrett, and A. K. Seth, *Physical Review Letters* **103**, 238701 (2009).
 - [76] J. G. Runge, *Phd thesis*, Humboldt University Berlin (2014).
 - [77] E. Olbrich, N. Bertschinger, and J. Rauh, *Entropy* **17**, 3501 (2015).
 - [78] A. B. Barrett, *Physical Review E* **91**, 052802 (2015).
 - [79] S. Wright, *The Annals of Mathematical Statistics* **5**, 161 (1934).
 - [80] T. VanderWeele, *Explanation in causal inference: methods for mediation and interaction* (Oxford University Press, Oxford, 2015).
 - [81] P. Spirtes, T. Richardson, C. Meek, R. Scheines, and C. Glymour, *Sociological methods & research* **27**, 182 (1998).
 - [82] K. J. Blinowska and M. Kaminski, *PloS one* **8**, e78763 (2013).
 - [83] S. L. Simpson, F. D. Bowman, and P. J. Laurienti, *Statistics Surveys* **7**, 1 (2013).
 - [84] J. F. Donges, *Ph.D. thesis*, Humboldt University Berlin (2012).
 - [85] M. E. J. Newman, *Networks: An Introduction* (Oxford University Press, Oxford, 2010).
 - [86] S. Bialonski, M. T. Horstmann, and K. Lehnertz, *Chaos: An Interdisciplinary Journal of Nonlinear Science* **20**, 13134 (2010).

- [87] J. Hlinka, D. Hartman, and M. Paluš, Chaos: An Interdisciplinary Journal of Nonlinear Science **22** (2012).
- [88] W. Liao, J. Ding, D. Marinazzo, Q. Xu, Z. Wang, C. Yuan, Z. Zhang, G. Lu, and H. Chen, Neuroimage **54**, 2683 (2011).
- [89] G. Deshpande, P. Santhanam, and X. Hu, NeuroImage **54**, 1043 (2011).
- [90] L. C. Freeman, Social Networks **1**, 215 (1979).
- [91] T. J. Ansell, P. D. Jones, R. J. Allan, D. Lister, D. E. Parker, M. Brunet, A. Moberg, J. Jacobeit, P. Brohan, N. A. Rayner, et al., Journal of Climate **19**, 2717 (2010).
- [92] E. Palmén and C. W. Newton, *Atmospheric circulation systems: Their structure and physical interpretation* (Academic Press, New York, 1969), 13th ed.
- [93] M. Vejmelka, L. Pokorná, J. Hlinka, D. Hartman, N. Jajcay, and M. Paluš, Climate Dynamics **44**, 2663 (2014).

Appendix A: Forward-selection as a causal reconstruction algorithm

A forward-selection algorithm alone cannot be used to reconstruct graphical models. The non-uniform embedding vector reconstructed with the scheme proposed in Refs. [14, 36, 41], therefore, can contain also non-causal drivers: In the first step of forward selection, the variable which maximizes the MI with Y is picked. Then causal drivers are iteratively determined based on how much information they contain *additionally* to the already chosen variables using CMI. A simple example demonstrating why this can select spurious drivers is

$$\begin{aligned} X_t &= a(Z_{t-1}^1 + Z_{t-1}^2) + \eta_t^X \\ Y_t &= c(Z_{t-2}^1 + Z_{t-2}^2) + \eta_t^Y, \end{aligned} \quad (\text{A1})$$

with Gaussian unit variance white noise processes $Z^{1,2}, \eta^{X,Y}$. Clearly, here Z^1 and Z^2 are the causal driving variables of Y at lag $t-1$ in the sense of Pearl, i.e., an intervention in Z^1 or Z^2 changes the distribution of Y while an intervention in X does not. But for positive c and $a > \frac{1}{\sqrt{2}}$ the MI between X_{t-1} and Y_t is larger than the MI between any of the $Z_{t-2}^{1,2}$ and Y_t . Thus, a non-causal variable is selected first which unnecessarily increases the dimension of the non-uniform embedding vector. By testing each variable again conditional on the remaining variables in the vector (backward-elimination), spurious drivers can finally be removed [36, 41–43].

Appendix B: Proofs of theorems

1. Proof of Inequality Theorem 1

The Inequality Theorem 1 can be proven similarly to the inequalities among ITY and MIT in Ref. [39]. To simplify notation, we drop the time indices and write X for $X_{t-\tau}$, Y for Y_t , and $\mathcal{C}_{X \rightarrow Y}$ for $\mathcal{C}_{X_{t-\tau} \rightarrow Y_t}$.

Proof. We define $\tilde{\mathcal{P}}$ to be the set of parents of both Y and the path nodes $\mathcal{C}_{X \rightarrow Y}$ (including X) that is not already included in the conditions of ITX $(\mathcal{P}_X, \mathcal{N}_X^Y, \mathcal{P}(\mathcal{N}_X^Y))$, i.e.,

$\tilde{\mathcal{P}} = (\mathcal{P}_Y \setminus \mathcal{C}_{X \rightarrow Y}, \mathcal{P}(\mathcal{C}_{X \rightarrow Y})) \setminus (\mathcal{P}_X, \mathcal{N}_X^Y, \mathcal{P}(\mathcal{N}_X^Y))$. Then it generally holds that $I(X; \tilde{\mathcal{P}} | \mathcal{P}_X, \mathcal{N}_X^Y, \mathcal{P}(\mathcal{N}_X^Y)) = 0$: Firstly, all paths arriving at X from the past are surely blocked (see Sect. III B) by \mathcal{P}_X because they contain the motifs $\rightarrow \blacksquare \rightarrow X$ or $\rightarrow \blacksquare \rightarrow X$ which are both blocked. Further, also contemporaneous sidepaths are blocked by $(\mathcal{N}_X^Y, \mathcal{P}(\mathcal{N}_X^Y))$ and there are also no directed causal paths from X to any node in $\tilde{\mathcal{P}}$ since, by definition, such a node would belong to $\mathcal{C}_{X \rightarrow Y}$. We now apply the chain rule on the (multivariate) CMI $I(X; (Y, \tilde{\mathcal{P}}) | \mathcal{P}_X, \mathcal{N}_X^Y, \mathcal{P}(\mathcal{N}_X^Y))$ twice:

$$\begin{aligned} I(X; (Y, \tilde{\mathcal{P}}) | \mathcal{P}_X, \mathcal{N}_X^Y, \mathcal{P}(\mathcal{N}_X^Y)) \\ = I(X; Y | \mathcal{P}_X, \mathcal{N}_X^Y, \mathcal{P}(\mathcal{N}_X^Y)) \\ + \underbrace{I(X; \tilde{\mathcal{P}} | \mathcal{P}_X, \mathcal{N}_X^Y, \mathcal{P}(\mathcal{N}_X^Y), Y)}_{\geq 0} \end{aligned} \quad (\text{B1})$$

$$\begin{aligned} = \underbrace{I(X; \tilde{\mathcal{P}} | \mathcal{P}_X, \mathcal{N}_X^Y, \mathcal{P}(\mathcal{N}_X^Y))}_{=0} \\ + I(X; Y | \tilde{\mathcal{P}}, \mathcal{P}_X, \mathcal{N}_X^Y, \mathcal{P}(\mathcal{N}_X^Y)) \end{aligned} \quad (\text{B2})$$

$$\begin{aligned} \Rightarrow I(X; Y | \tilde{\mathcal{P}}, \mathcal{P}_X, \mathcal{N}_X^Y, \mathcal{P}(\mathcal{N}_X^Y)) \\ = I(X; Y | \mathcal{P}_Y \setminus \mathcal{C}_{X \rightarrow Y}, \mathcal{P}(\mathcal{C}_{X \rightarrow Y}), \mathcal{N}_X^Y, \mathcal{P}(\mathcal{N}_X^Y)) \\ \geq I(X; Y | \mathcal{P}_X, \mathcal{N}_X^Y, \mathcal{P}(\mathcal{N}_X^Y)). \end{aligned} \quad (\text{B3})$$

□

2. Further information-theoretic properties

Some further fundamental properties of information-theoretic quantities are important for the coupling strength autonomy theorems. The data processing inequality [4] states that

$$I(X; f(Y) | Z) \leq I(X; Y | Z), \quad (\text{B4})$$

i.e., manipulating Y by some function f can only reduce the shared information. Note, however, that equality holds for smooth uniquely invertible transformations such as linear rescalings of X , Y or Z under which CMI is invariant [51]. For random variables Y and W and an arbitrary function f we have that

$$\begin{aligned} H(Y + f(W) | W) &= \int p(w) H(Y + f(W) | W = w) dw \\ &= \int p(w) H(Y | W = w) dw \\ &= H(Y | W), \end{aligned} \quad (\text{B5})$$

because $f(W)$ for $W = w$ is a fixed constant and entropies are translationally invariant. In particular, $H(f(W) | W) = 0$. This property also holds for the joint entropy and with another arbitrary function g it follows for CMI that

$$I(X + g(Z); Y + f(W)|Z, W) = I(X; Y|Z, W). \quad (\text{B6})$$

Also here, $I(X; f(W)|W) = 0$. Last, conditions that are conditionally independent of X and Y given Z can be dropped:

$$\begin{aligned} X \perp\!\!\!\perp W|Z \text{ and } Y \perp\!\!\!\perp W|Z \\ \implies I(X; Y|Z, W) = I(X; Y|Z), \end{aligned} \quad (\text{B7})$$

which can be easily derived from $I((X, Y); W|Z) = 0 \implies H(X, Y|Z, W) = H(X, Y|Z)$ and correspondingly for the marginals.

3. Proof for momentary information transfer along paths

Also here, to simplify notation we drop the time indices and write X for $X_{t-\tau}$, Y for Y_t , and $\mathcal{C}_{X \rightarrow Y}$ for $\mathcal{C}_{X_{t-\tau} \rightarrow Y_t}$. In the theorem, we denoted those parents of Y that are in the path nodes $\mathcal{C}_{X \rightarrow Y}$ defined in Eq. (21) as $\mathcal{P}_Y^{\mathcal{C}} = \mathcal{P}_Y \cap \mathcal{C}_{X \rightarrow Y}$ and correspondingly for other path nodes $\mathcal{P}_i^{\mathcal{C}}$. Also note that X is included in the set of path nodes.

Proof. We insert the dependencies assumed for X and Y in Eq. (41) in the definition of MITP (Eq. (24)):

$$\begin{aligned} I_{X \rightarrow Y}^{\text{MITP}} \\ = I(X; Y | \mathcal{P}_Y \setminus \mathcal{C}_{X \rightarrow Y}, \mathcal{P}(\mathcal{C}_{X \rightarrow Y}), \mathcal{N}_X^Y, \mathcal{P}(\mathcal{N}_X^Y)) \end{aligned} \quad (\text{B8})$$

$$\stackrel{\text{Eq. (41)}}{=} I(g_X(\mathcal{P}_X) + \eta^X; f_Y(\mathcal{P}_Y^{\mathcal{C}}) + g_Y(\mathcal{P}_Y \setminus \mathcal{P}_Y^{\mathcal{C}}) + \eta^Y | \mathcal{P}_Y \setminus \mathcal{C}_{X \rightarrow Y}, \mathcal{P}(\mathcal{C}_{X \rightarrow Y}), \mathcal{N}_X^Y, \mathcal{P}(\mathcal{N}_X^Y)) \quad (\text{B9})$$

$$\stackrel{\text{Eq. (B6)}}{=} I(\eta^X; f_Y(\mathcal{P}_Y^{\mathcal{C}}) + \eta^Y | \mathcal{P}_Y \setminus \mathcal{C}_{X \rightarrow Y}, \mathcal{P}(\mathcal{C}_{X \rightarrow Y}), \mathcal{N}_X^Y, \mathcal{P}(\mathcal{N}_X^Y)). \quad (\text{B10})$$

In the theorem, f_Y is assumed linear and we also assumed all other path nodes $W^{(i)} \in \mathcal{C}_{X \rightarrow Y}$ to linearly depend on each other by Eq. (42), where dependencies on external nodes were only assumed additive. Then,

$$\begin{aligned} I_{X \rightarrow Y}^{\text{MITP}} \stackrel{\text{Eq. (B6)}}{=} I(\eta^X; f(\eta^X, \cup_i \eta^i) + \eta^Y \\ | \mathcal{P}_Y \setminus \mathcal{C}_{X \rightarrow Y}, \mathcal{P}(\mathcal{C}_{X \rightarrow Y}), \mathcal{N}_X^Y, \mathcal{P}(\mathcal{N}_X^Y)), \end{aligned} \quad (\text{B11})$$

for some linear function f yielding Eq. (43). Now under the “no contemporaneous dependency”-condition Eq. (40) we can drop the conditions due to Eq. (B7),

$$I_{X \rightarrow Y}^{\text{MITP}} \stackrel{\text{Eq. (B7)}}{=} I(\eta^X; f(\eta^X, \cup_i \eta^i) + \eta^Y), \quad (\text{B12})$$

yielding Eq. (44). Note that due to Markovity the dynamical noise is i.i.d. and, since $0 < \tau_i < \tau$, it holds that $(\eta^X, \eta^Y) \perp\!\!\!\perp \eta^i \forall i$ and $\eta^X \perp\!\!\!\perp \eta^Y$. \square

This proof also includes the proof for the MIT coupling strength autonomy theorem as a special case, but in a much shorter form than in Ref. [39]: If $\mathcal{C}_{X_{t-\tau} \rightarrow Y_t} = \{X_{t-\tau}\}$, and under the “no sidepath”-constraint in Ref. [39], the conditions on the neighbors can be dropped and MITP collapses to MIT. Since then also $f(\eta_{t-\tau}^X, \cup_i \eta_{t-\tau}^i) = f(\eta_{t-\tau}^X)$, Eq. (44) reduces to the same form as in Ref. [39].

4. Proof for momentary interaction information

Using the same assumptions as for Theorem 2, the dependencies of momentary interaction information between X , Y and intermediate processes $\mathbf{W} = (W_{t-\tau_1}^{(1)}, W_{t-\tau_2}^{(2)} \dots) \in \mathcal{C}_{X_{t-\tau} \rightarrow Y_t} \setminus \{X_{t-\tau}\}$ indexed by j can be simplified exploiting the same arguments as above.

Proof.

$$\begin{aligned} \mathcal{I}_{X \rightarrow Y | \mathbf{W}}^{\text{MI}} \\ = \mathcal{I}(X; Y; \mathbf{W} | \mathcal{P}_Y \setminus \mathcal{C}_{X, Y}, \mathcal{P}(\mathcal{C}_{X \rightarrow Y}), \mathcal{N}_X^Y, \mathcal{P}(\mathcal{N}_X^Y)) \end{aligned} \quad (\text{B13})$$

$$\stackrel{\text{Eq. (B6)}}{=} \mathcal{I}(\eta^X; f(\eta^X, \cup_i \eta^i) + \eta^Y; \{\eta^j + f_j(\eta^X, \cup_{i \neq j} \eta^i)\}_j | \mathcal{P}_Y \setminus \mathcal{C}_{X \rightarrow Y}, \mathcal{P}(\mathcal{C}_{X \rightarrow Y}), \mathcal{N}_X^Y, \mathcal{P}(\mathcal{N}_X^Y)) \quad (\text{B14})$$

$$\stackrel{\text{Eq. (B7)}}{=} \mathcal{I}(\eta^X; f(\eta^X, \cup_i \eta^i) + \eta^Y; \{\eta^j + f_j(\eta^X, \cup_{i \neq j} \eta^i)\}_j), \quad (\text{B15})$$

where the last step is valid only under the “no contemporaneous dependency”-condition Eq. (40) giving Eq. (46) with linear functions f, f_j . \square